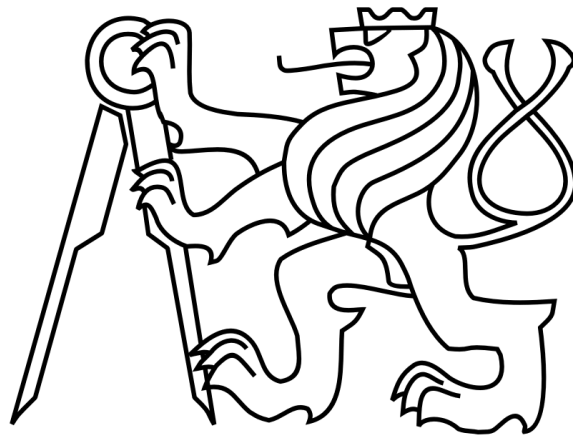


Software Tools for Digitization and Postprocessing of Archival Film Materials

Programové vybavení pro digitalizaci a následné zpracování archivních filmových
materiálů

Timur Sibgatullin

August 15, 2022



Czech Technical University in Prague

Supervisor: **Ing. Karel Fliegel, Ph.D.**
Department of Radioelectronics
Faculty of Electrical Engineering
Czech Technical University in Prague
Technická 2, Prague 6, 166 27



BACHELOR'S THESIS ASSIGNMENT

I. Personal and study details

Student's name: **Sibgatullin Timur** Personal ID number: **483622**
Faculty / Institute: **Faculty of Electrical Engineering**
Department / Institute: **Department of Radioelectronics**
Study program: **Electronics and Communications**

II. Bachelor's thesis details

Bachelor's thesis title in English:

Software Tools for Digitization and Postprocessing of Archival Film Materials

Bachelor's thesis title in Czech:

Programové vybavení pro digitalizaci a následné zpracování archivních filmových materiálů

Guidelines:

Give an overview of advanced digitization methods and postprocessing techniques for archival film materials. Focus on workflows utilizing flat copy scanning of positive and negative film materials with digital single-lens reflex cameras. Implement software tools to demonstrate the described methods and verify their performance using available image samples.

Bibliography / sources:

- [1] Jícha, M. a kol., Živý film: Digitalizace filmu Metodou DRA, Lepton studio, 2016.
- [2] ISO/TR 19263-1:2017, Photography - Archiving systems - Part 1: Best practices for digital image capture of cultural heritage material.
- [3] ISO 19264-1:2021, Photography - Archiving systems - Imaging systems quality analysis - Part 1: Reflective originals.

Name and workplace of bachelor's thesis supervisor:

Ing. Karel Fliegel, Ph.D. Department of Radioelectronics FEE

Name and workplace of second bachelor's thesis supervisor or consultant:

Date of bachelor's thesis assignment: **11.02.2022** Deadline for bachelor thesis submission: **15.08.2022**

Assignment valid until: **30.09.2023**

Ing. Karel Fliegel, Ph.D.
Supervisor's signature

doc. Ing. Stanislav Vitek, Ph.D.
Head of department's signature

prof. Mgr. Petr Páta, Ph.D.
Dean's signature

III. Assignment receipt

The student acknowledges that the bachelor's thesis is an individual work. The student must produce his thesis without the assistance of others, with the exception of provided consultations. Within the bachelor's thesis, the author must state the names of consultants and include a list of references.

Date of assignment receipt

Student's signature

Contents

Abbreviations and glossary	7
Introduction	9
1 Digital Imaging	11
1.1 Digital vs. film cameras	11
1.2 CCD Flatbed, drum and CMOS scanners	12
1.3 Histogram	13
1.4 Intensity transformations	13
1.4.1 Gamma encoding	14
1.4.2 Log encoding	15
1.5 Existing solutions of film digitization using a digital camera	16
1.5.1 Phase One	16
1.5.2 Semi-professional and amateur solutions	16
1.5.3 Price comparison	17
1.6 Macro photography	19
2 Film density	21
2.1 Definition of density	21
2.2 Characteristic curve	22
2.3 Spectral conditions for color film	23
2.3.1 Spectral response	23
2.3.2 Color separation	24
2.3.3 Types of spectral responses	25
2.4 Spectral conditions for monochrome film	26
2.5 Densitometer	27
2.6 Dedicated motion picture scanners	27
2.6.1 Illumination source	27
2.6.2 Sensor pattern	27
2.6.3 Dynamic range	28
2.7 Encoding density	28
2.7.1 Cineon and DPX	28
2.7.2 Log. formats in DSLR	30
2.7.3 Using density information	30
3 HDR	31
3.1 Multiple-exposure HDR	31
3.2 HDR storage formats	32
3.2.1 Radiance/HDR format	32
3.2.2 TIFF	32
3.2.3 OpenEXR	33
3.2.4 Comparison of formats	33

4	Optical Aberrations	36
4.1	Distortion	36
4.2	Vignetting	36
4.3	Chromatic aberration	38
4.4	Spherical aberration	39
5	OECF and MTF	40
5.1	Opto-electronic conversion function	40
5.2	Modulation transfer function	40
6	Sample acquisition, digitizing and performance evaluation	42
6.1	Film samples	42
6.2	Digitizing equipment	43
6.3	Flat-field correction	47
6.4	OECF measurement	48
6.5	MTF/SFR measurement	55
6.6	System with analog + digital camera	61
7	Linear density encoding and digital printing	69
7.1	Transfer function for linear density encoding	69
7.2	Process of linear density encoding	70
7.3	Proposed digital printing process	71
7.4	Encoding and printing process	73
8	Conclusions	80
	Attachments	82

Acknowledgements

I would like to thank Ing. Karel Fliegel, Ph.D. for his time, patience, faith, and resourcefulness.

Abstract

This work explores the necessary knowledge and prerequisites for *digitizing film materials* using a digital single-lens reflex camera, such as the concepts of digital imaging, optical density, logarithmic encoding, HDR (High dynamic range) and optical aberrations. Based on that knowledge, samples of negative film were acquired with DSLRs in three different setups. *OECF* (Opto-electronic conversion function) and *MTF* (Modular transfer function) were utilized to evaluate performance of two DSLRs and compare them to those of a flatbed scanner and a dedicated film scanner. *OECF* and samples was also used to implement and demonstrate software tools for logarithmic transfer function to encode density linearly. Linearly encoded density was then used to implement and demonstrate a semi-automated software solution for a proposed 'digital printing' method of the film, which considers properties of the photographic paper.

Keywords: Film, DSLR, Scanner, Digitization, MTF, OECF, Nikon D700, Canon EOS 5D Mark IV.

Abstrakt

Tato práce se zabývá potřebnou znalostí a předpoklady pro *digitalizaci filmových materiálů* s použitím digitálních zrcadlovek, jako jsou například koncepty digitálních obrazů, optické hustoty, logaritmického kódování, HDR (Vysoký dynamický rozsah) a optických vad. V souladu s touto informací byly následně pořízeny vzorky negativního filmu s pomocí zrcadlovek ve třech různých konfiguracích. *OECF* (Opto-elektronická konverzní funkce) a *MTF* (Modulární přenosová funkce) byly použity pro zhodnocení dvou zrcadlovek a jejich porovnání se stolním skenerem a filmovým skenerem. *OECF* a vzorky byly také použity pro implementaci a demonstraci softwarového vybavení pro lineární kódování hustoty, využívajícího logaritmickou přenosovou charakteristiku. Následně byla lineárně zakódovaná hustota využita pro implementaci a demonstraci softwarového řešení navrženého 'digitálního tisku', který využívá informaci o vlastnostech fotonapáje.

Klíčová slova: Film, Zrcadlovka, Digitalizace, MTF, OECF, Nikon D700, Canon EOS 5D Mark IV.

Affidavit

I hereby affirm that this Bachelor's Thesis represents my own written work and that I have used no sources and aids other than those indicated. All passages quoted from publications or paraphrased from these sources are properly cited and attributed.

Čestné prohlášení

Prohlašuji, že jsem předloženou práci vypracoval samostatně a že jsem uvedl veškeré použité informační zdroje v souladu s Metodickým pokynem o dodržování etických principů při přípravě vysokoškolských závěrečných prací.

Signature:.....

Abbreviations and glossary

Following is glossary and a list of abbreviations commonly used throughout this work.

5D: A digital camera, Canon EOS 5D Mark IV.

bpc: Bits per channel/bits per color channel/bits per color component.

BPP: Total bits per pixel. In some instances, such as in LogLuv encoding, it wouldn't make sense to state the bits per color channel.

CRI: Color rendering index, describes a light source's ability to reproduce colors. On ascending scale from 0 to 100.

Coolscan IV: Nikon Coolscan IV, a dedicated film scanner.

CV, IV: Code value or intensity value of a pixel.

CA: Chromatic aberration, failure of different light wavelengths to concentrate on the same plane/point.

CRI: Color rendering index, describes how well a light source can reproduce colors of an illuminated object.

D_{min} : The minimum density that a given film can achieve. In case of negative film, it is the density of film that has not been subjected to exposure. May also be called base density in certain sources.

D_{max} : The maximum density that a given film can achieve. In case of reversal film, it is the density of film that has not been subjected to exposure.

D700: Nikon D700, full frame 12MP camera.

DoF: Depth of field is the area where objects appear plausibly sharp.

EV: Exposure value follows the same exact logarithmic pattern as stops, but EV's are assigned to specific combination of shutter speed and f-number.

FFC: Flat field correction, an blank image of the illuminating source is taken and used to compensate for uneven illumination and vignetting of the camera.

f-number, f-stop, f/: f-number N represents the ratio of the focal length f and aperture diameter D : $N = \frac{f}{D}$.

IN/IP: Intermediate negative or positive. Intermediate stages of film during the creation of motion pictures. Color correction is typically performed on the interpositive, while the internegative serves as the printing source for print film, which is then distributed into cinemas.

ISO: ISO (formerly also ASA) represents sensor sensitivity (gain) in the case of digital cameras and film speed in the case of film. Higher ISO means higher gain and faster reaction to exposure.

MTF, SFR: Modulation transfer function and spatial frequency response, both describe an optical system's response to various spatial frequencies.

OCN: Original camera negative. When shooting motion pictures with film, the stock in the camera is in overwhelming amount of cases a negative, OCN refers to that copy which was used in the film camera.

OECF: Opto-electronic conversion function establishes a relationship between input luminance and digital output CVs.

Output/display referred: Data storage methods/workflows focused on images being correctly displayed on monitors.

Print paper/ print stock: Print paper is the final stage of the photograph. It is produced when a strip of film is enlarged, exposed and projected onto a larger medium. Similarly, print stock is the final analog storage medium of motion pictures, it is the stock that is sent to cinemas for viewing. Unlike original negatives and intermediate films, it is meant to be viewed by humans and this is often higher in contrast.

SA: Spherical aberration. Failure of parallel light beams coming from the same plane to be properly in focus due to the shape of the lens.

Scene referred: Data storage methods/workflows focused on preserving original scene luminance values and their correct transformations between color spaces.

Shutter speed, exposure time: Describes for how long the sensor is exposed to light.

Stop: An increase or decrease of 1 stop in photography refers to doubling or halving the amount of light falling on the sensor and the ISO setting. To achieve an increase of 1 stop, we must double the exposure time or double the ISO setting or increase the f-number by $\sqrt{2}$. Stops are a logarithm with a base of 2.

V550: Epson Perfection V550, a flatbed scanner.

Introduction

Film contains fine detail that is only limited by the size of individual silver halide crystals, or other image forming compounds, not the amount of pixels. Unlike digital images, however, film physically deteriorates with time. At some point, in order to preserve the film, it must be copied onto a new medium. Not including reliability, digital imaging provides several advantages, such as immediate color correction, copying and interchanging between people/devices. For those reasons, film is often digitized. Among the first devices to do so were drum scanners, that are nowadays expensive to buy, lengthy to operate and hard to find. Dedicated film scanners and flatbed scanners are more common, cheaper and easier to operate, but don't match the resolution of a drum scanner. Digital photography is also emerging as a solution to digitizing film, among professionals and amateurs alike. With increasing capabilities of digital *CMOS* sensors, digital cameras are rivaling scanners not only in terms of speed and efficiency, but also in terms of image quality and dynamic range. Companies, namely *Phase One*¹, are making dedicated hardware for this purpose, which can cost as much as millions of Czech crowns. Meanwhile, lesser known companies like *Valoi*² offer equipment for scanning film at home.

Compared to a new strip of film, archive film materials are more faded, brittle, and are more likely to contain scratches and other physical signs of deterioration. However, the ideas behind scanning archive and new film stock are the same - a digital camera, an illuminated table/copy stand with an acceptable *CRI*, a film holder, perfect alignment of film and sensor planes, and photo editing software. For that reason, all things said that apply to new film stocks, also apply to archive film material. The main difference is that archive film material must be handled with more care, and additional factors, like color separation, might be considered, but new film will benefit from those as well.

While manufacturers and operators of motion picture film scanners (that also use *CMOS* sensors) follow strict industry standard procedures (e.g. *Cineon*), scanning of still images using a digital camera lacks those guidelines, especially procedures involving linear encoding of density. For those reasons, I find it appropriate to gather information necessary to digitize film using a digital camera, perform experiments in accordance with that information, compare the performance of a digital camera to performance of a flatbed scanner, and, finally, to demonstrate a digitization workflow that would involve linear encoding of densities.

The work is divided into following sections: for theoretical base, the work will explore the core concepts of *digital imaging* (section 1), including the description of necessary software, hardware, and overview of existing digitization methods. Then, *film density* will be discussed (section 2), along with methods of measuring density and the potential uses of linearly encoded density in an image file. Given film's high dynamic range and certain devices' inability to capture that range in one photo/certain file formats inability to store it, some knowledge of *HDR* photography and formats will be of use (section 3). To complete the theoretical part, I will also mention *optical aberrations* (section 4), some of which significantly impact the quality/faithfulness of the scan and thus must be corrected/considered before or after taking the photograph.

¹<https://digitization.phaseone.com>

²<https://www.valoi.co>

To evaluate the performance of DSLR scanning and compare it to other mean of scanning, I will use OECF (Opto-electronic conversion function) and MTF (Modulation transfer function). Explanation of OECF and MTF are in section 5. After describing the used setups and equipment, OECF and MTF of multiple devices is tested - two DSLRs, a flatbed scanner and a dedicated film scanner (section 6). Then, using data from OECF and acquired negative film samples, I will logarithmically encode said scanned samples to contain linear density representation. With logarithmically encoded data, it may be possible to imitate a printing process which considers and utilizes properties of a printing paper (section 7).

1 Digital Imaging

The very first theoretical base required for this work is digital imaging. This section discusses the properties of digital cameras, digital files, flatbed CCD scanners and intensity transformations. Finally, I will provide a summary of existing scanning workflows, such as PhaseOne's professional solution or several semi-professional solutions, and compare the estimates of their price ranges.

1.1 Digital vs. film cameras

Digital and film cameras share many similarities to a point where a film camera can be transformed into a digital device using a *digital back* - a digital sensor mounted onto a film camera, into the place where the film roll would originally be. The optical path is virtually identical and concepts such as focus, f-number and exposure time apply to both types of devices. Autofocus is achieved using either *phase detection* (DSLR, mirrorless digital, and film cameras) or *contrast detection* (DSLR in live view and mirrorless digital cameras) [1]. A digital camera's ISO expresses the amount of gain of the circuit, whereas film's ISO refers to the reaction speed of the chemicals. In both cases, higher ISO also constitutes more perceptible grain/noise [2].

The mediums differ in how they write and store information. Film's resolution is theoretically only limited by the size of individual *image-forming chemical compounds*. Fully capturing the entirety of the **grain structure** (10 - 30 μm) on a 35 mm film theoretically necessitates a horizontal resolution of around 128K [3]. On the other hand, digital camera sensors (mostly CMOS) have a predetermined resolution in *pixels*, which works in tandem with an optical low-pass filter to prevent aliasing (Moiré pattern) [1]. The amount of visual information (including grain) on a 35 mm film is sometimes higher than a regular consumer-grade camera can capture, but the task is often not to preserve all the information on film, it is to establish a threshold beyond which it becomes unnecessary or impractical to increase the resolution. In the case of motion picture film stock, the industry standard scanning resolution for 35 mm film is 6K, which is then downsampled to 4K [3][1]. We must keep in mind that unlike a **sequence** of motion picture images, still photographs are often enlarged and appreciated for the detail, thus requiring higher resolution, however consumer digital cameras come with their own pixel resolution that cannot be changed.

File formats outputted by digital cameras nowadays are either *RAW formats* (.cr2, .nef) and/or *JPEGs* of varying quality [4]. RAW files have the benefit of containing all the luminance values captured by the sensor, while DCT compressed JPEG files offer noticeably smaller sizes at the cost of information (might not be perceptible at first, but leaves no headroom for manipulation). RAW files have a bit depth of 12, 14 or 16 bpc, whereas JPEG can only output 8 bpc files [4]. Digital sensors commonly have a mosaic pattern (mostly the Bayer Pattern), meaning any given pixel can capture either red, blue, or green colors [4]. RAW data therefore needs to be demosaiced, that is, the remaining two color components of a pixel have to be interpolated based on the information from the neighboring pixels. This is why RAW files require a RAW processing engine, such as *Adobe Camera Raw*³ or *Capture One*⁴. A lossless format, on which most RAW formats are based, is *TIFF*. Those can store the raw pixel values from the sensor as well, with the difference of added demosaicing and baked-in white balance. All three formats support *EXIF metadata*, which contains

³<https://helpx.adobe.com/camera-raw/using/supported-cameras.html>

⁴<https://www.captureone.com/en>

camera settings used to take the image (ISO, shutter speed and f-number) [4].

1.2 CCD Flatbed, drum and CMOS scanners

In contrast to digital cameras, flatbed scanners use a light source and a series of optical elements, which reflect the light from the said light source onto the scanned object, and then onto a CCD array, one line at a time [5]. The pixel arrays for three color components are separate, and some scanners can scan in B&W in greater precision than in color, as will be shown in the practical part of this thesis (section 6.5). To scan film, the scanner needs to operate in transmissive mode, shown in figure 1.2.1. Some CCD scanners are made specially for films, such as Nikon Coolscan 9000⁵. Given their specialization, they may offer superior quality to conventional flatbed scanners, but they are becoming increasingly uncommon. The parameters of scanners are not given directly in pixels, but in dpi – dots per inch. Higher dpi constitutes not only better quality, but higher scanning times. The advantage a flatbed scanner has over a digital camera is that it requires little to no setup to operate, and software such as VueScan⁶ and SilverFast⁷ can automatically color correct the images, including negative film. Another edge over cameras is that they offer better light isolation to ensure we are scanning mostly *transmitted* light, not reflected light. Some scanners go as far as detecting dust/scratches, for example using the infrared portion of electromagnetic spectrum - it passes through film, but is absorbed by dust/scratches. That feature is also integrated in software solutions, e.g. aforementioned SilverFast⁸. The main disadvantage is the speed of operation, once a camera is set up, it can scan images at a much faster rate. PhaseOne⁹'s devices can scan at advertised speed of approximately 1 image per second [6], while, for example, scanning film in a flatbed scanner took me a minute per image at 2400dpi.

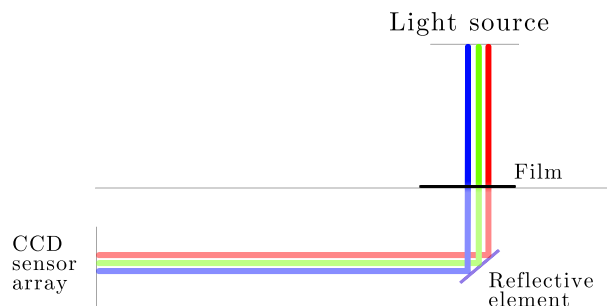


Figure 1.2.1: The principle of a flatbed CCD scanner operating in transmission mode. Inspired by [5].

⁵https://www.nikon.cz/cs_CZ/product/discontinued/coolscan/2011/super-coolscan-9000

⁶<https://www.hamrick.com/>

⁷<https://www.silverfast.com/highlights/negafix/en.html>

⁸<https://www.silverfast.com/about-silverfast-why-scanning-basics-of-scanning/why-silverfast/silverfast-feature-highlights/isrd-dust-scratches-removal-eliminate-defects-with-infrared-channel/>

⁹<https://digitization.phaseone.com>

A drum scanner offers superior image quality to a flatbed scanner, but those are slow to operate and hard to come by nowadays. Furthermore, archive film material should be protected from physical strain, rendering drum scanners useless in certain scenarios.

There are also "scanners" using CMOS technology, but they do not scan the image progressively, line by line, instead, they capture the entire image at once, just like a digital camera would. An example of that would be the *REFLECTA X66-Scan*¹⁰.

1.3 Histogram

An image histogram is a discrete function that displays the number of pixels with a particular *CV* (Code Value) [4]. It may be interpreted as a discrete probability density function. Histogram is most useful as a visual aid, as it shows the used range of lightness and possible clipping values. It allows to predict and display the impact of intensity transformations (for example spikes or gaps in histogram mean the tonal range was most likely compressed or expanded). Its statistical nature can be used for transformations as well, for example *histogram equalization* [7], to increase contrast.

1.4 Intensity transformations

Intensity transformations change CVs of individual pixels in the spatial domain with transfer functions, which establish a relationship between input and output CVs. It may be done for aesthetic purposes, but also for preservation of visual information, for example *gamma correction* [4], *log transform* [8] or *inversion* (negative to positive). In commercial software, the most used tools to visualize and perform intensity transformations are commonly called *levels* and *curves* [4]. Another way to characterize a transformation is using an LUT. An LUT is a one-dimensional or three-dimensional (for color images) array that assigns an output CV to an input CV [8], [1]. Intensity transformations important for this work are shown in figure 1.4.1.

¹⁰<https://www.fotoskoda.cz/reflecta-x66-scan-svitek-kinofilm-skener/>

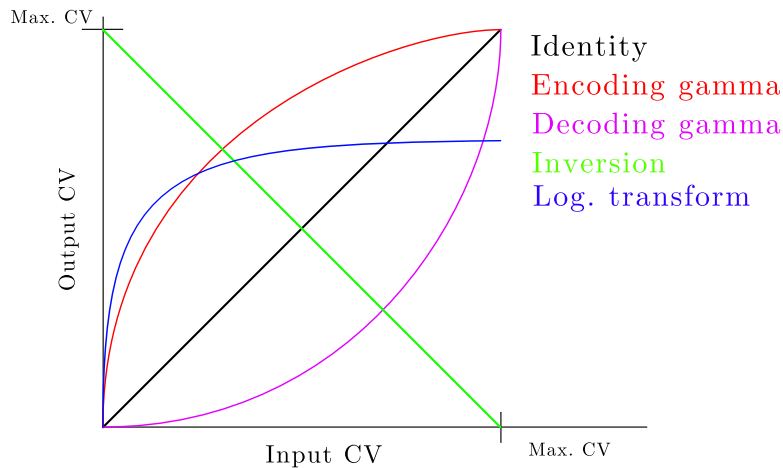


Figure 1.4.1: Intensity transformations mentioned throughout this work. The gamma and log. transforms are not using any specific constants, the picture is meant for illustration purposes only. Depicted transformations will be used in the practical part, and will be described in more detail there.

1.4.1 Gamma encoding

Encoding image files linearly, as they were photographed, would constitute perceptible loss of detail in the darker areas of the image if the quantization step is not small enough. It is because human perception of light intensity seems to follow power-law or logarithmic pattern, meaning changes in lower light intensities are more noticeable than changes in higher light intensities [9]. Even if loss of detail does not occur at first, there is little to no headroom for transformations. It is for those reasons that gamma encoding is used in images; allocating more CVs to lower light intensities at the expense of higher light intensities to increase stored visual information at the same bit depth, and to allow computers to work with images linearly, applying transformations as they will be seen by humans. Comparison of linear and gamma encoding is shown in figure 1.4.2. To be gamma corrected, the CVs usually must be normalized. Encoding γ is always a value lower than 1. For displaying the image, it then needs to be gamma decoded. Decoding γ is calculated as encoding γ over 1, therefore it is always bigger than 1.

$$CV_{OUT_{Normalized}} = CV_{IN_{Normalized}}^{\gamma} \tag{1.4.1}$$

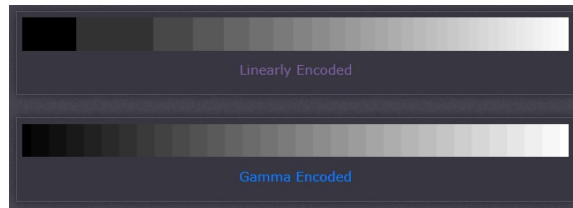


Figure 1.4.2: Allocated CVs for linear (upper) and gamma (lower) encoded data. Image courtesy of [9].

Unlike log encoding, gamma encoding is not noticed by the user. In certain scenarios we need to preserve the linear RAW data from the sensor that has not been gamma encoded, for example to measure the sensor’s OECF.

1.4.2 Log encoding

Logarithmic transformations follow a similar principle as gamma transformations, the log curve maps more CVs to lower intensities at the expense of higher intensities. Log encoding is used in digital cameras, such as Canon’s C-Log¹¹, ARRI’s LogC, Nikon’s N-Log¹² and Sony’s S-Log¹³, to preserve and map a greater dynamic range [10]. Log encoded images appear low in contrast, because they contain said dynamic range and are expected to be edited manually or transformed using 3D LUTs supplied by manufacturers. Log transformations are also used by Cineon and DPX format to linearly encode densities. That will be further discussed in the Cineon and DPX subsection with illustrations (section 2.7.1).

¹¹<https://www.canon.cz/cameras/eos-5d-mark-iv/canon-log-gamma/>

¹²https://www.nikonimgsupport.com/eu/BV_article?articleNo=000042504&configured=1&lang=cs

¹³<https://www.sony.com/electronics/support/articles/00145908>

1.5 Existing solutions of film digitization using a digital camera

This subsection provides an overview of professional (Phase One) and semi-professional/amateur methods (Nick Carver [11], Kyle McDougall [12]) of digitizing film with a digital camera, including cost estimates and comparison to other means of film digitization, such as drum scanner, flatbed scanner and dedicated film scanner. I was not able to find any performance metrics such as MTF from these sources.

1.5.1 Phase One

Phase One, the creator of the photo editing software *Capture One*, is the most known company that produces devices specifically for professionally digitizing archive material, including film. Their range of products includes camera systems, optics, Capture One Cultural Heritage software, film carriers and *AutoColumn* copy stands (in collaboration with *Cambo*, *Kaiser*, *Digital Transitions*).

Their *iXH 150 MP* camera system was designed to capture A0 size objects at the resolution of 300 ppi. The PPI-Assist function in Capture One CH measures the ppi based on the distance of used camera from the AutoColumn stand. The distance itself can then be adjusted from software. *iXH 150 MP* can be used either with 72 mm *Phase One RS* lens or *Schneider Kreuznach 120 mm lens*. For macro photography, the 120 mm lens can be outfitted with 21 mm and 42 mm *extension tubes*. *iXG 100 MP* too comes with 72 mm and 120 mm Schneider Kreuznach lenses. All the lenses mentioned above are advertised as achromatic. The imaging sensors are in 3 variants – normal, achromatic, and wide spectrum - for multispectral imaging purposes. Achromatic in this case means monochrome imagery, i.e., lack of a Bayer pattern. Both sensor sizes are medium format, meaning 53.4 by 40 mm. The output files can be 14 or 16 bpc RAW. Cultural Heritage Solution Guide also advertises the modular XF Camera System, which has a separate body, viewfinder, digital back, and lens. The IQ range of digital backs for XF too have a resolution of 150 MP and 100 MP and the lens range from 45 mm to 150 mm, with 45 mm having a f/3.5 aperture and the rest a f/2.8. All camera systems use fixed focal length lenses. Text above is a summary of information provided in [6].

1.5.2 Semi-professional and amateur solutions

It is not rare nowadays to see enthusiasts digitizing film using their own setup of a digital camera and illuminated copy stand. They might not use objective metrics, but their opinion still might be an indicator of what equipment should be used and how it performs in comparison to other means of digitizing film. One photographer for example went through the trouble and compared a DSLR with a flatbed scanner (*Epson Perfection V750* at 4800ppi) and a drum scanner [11]. The scanned material was a color negative and color reversal film. The DSLR used to perform the scan was a *Canon EOS 6D* with f/11 aperture and 100 mm focal length, stationed on a tripod above an illumination table. It is important to point out that the rest of the illumination table (the part not used for the film) was likely not covered properly to avoid light spill, which reduces the range of densities the DSLR can effectively capture. Since the film was too large to be photographed in one frame, multiple shots were taken and then stitched together. According to the author, the DSLR and drum scanner outperformed the flatbed scanner when it came to dynamic range and sharpness. Digital camera had the most visible dust present, whereas flatbed scanners usually have automatic dust detection and removal function using IR light. The author also had trouble recovering desired color from the DSLR scan however, while noting the convenience of Silverfast's *Negafix* feature,

which inverts color negatives with the type of film and film speed used. He pointed out that the workflow using the DSLR was the slowest, mostly due to the time it takes to set things into the right position. This suggests systems using DSLRs that are not as automated as Phase One’s solution should be set up and then minimally physically manipulated with, to optimize workflow.

Another photographer [12] used a *Fujifilm X-T4*, a 24 mm sensor camera mounted with a 60 mm f/2.8 lens. He compared it to a dedicated film scanner, *Nikon Coolscan 9000*, and *Epson 4990*, a flatbed scanner. This time, the film was held in a special carrier blocking the surrounding light. The carrier was supplied to the author by *VALOI* among other accessories, most importantly the copy stand, a diffuser for uneven illumination and a light [13]. When scanning medium-format images, dedicated Nikon film scanner contained the most detail and the mirrorless digital camera perceptibly outperformed the flatbed scanner, both in detail and dynamic range. Upon scanning 35mm film, though, the DSLR came very close in detail and dynamic range to Nikon Coolscan 9000.

Plug-ins for photo editing software such as *Negative Lab Pro* [14] or *ColorPerfect*¹⁴ make the workflow faster by inverting the RAW negative images and automatically color correcting the film.

1.5.3 Price comparison

I did a price comparison of methods mentioned above (in June 2022), but it’s worth mentioning that it is only a rough estimate, as prices naturally fluctuate and in certain cases are not even available on websites.

Capture One’s XF camera system equipped with an *150 MP IQ4* digital back, without lens, has a price of approximately 1,200,000 CZK [15]. Leasing is available too. A *45 mm Phase One Schneider Blue Ring* lens advertised in the Cultural Heritage Solution Guide costs an additional 160,000 CZK [16]. I was not able to find the price of the copy stand, but it is reasonable to assume that custom-built automated copy stands will not come cheap. Price of Capture One is negligible at this scale.

A full-frame digital camera body starts at approx. 25,000 CZK (Canon EOS RP) and can escalate to 70,000-80,000 CZK (Canon EOS 5D Mark IV, Nikon D850) or even beyond 120,000 CZK (LEICA, SONY Alpha A9 II). Prices were taken from the website FotoSkoda¹⁵. The highest prices are warranted by features not usually needed for film digitizing, like the number of auto-focus points and the speed of auto-focus. The jump from lowest prices to middle prices is justified by increased pixel count and dynamic range, meaning a camera in the 5D Mark IV’s price range should suffice. A full scanning kit for DSLRs by Valoi costs 15,000 CZK [13]. A more professional solution, a *Kaiser Copylizer* with LED illumination would cost 100,000 CZK [17], with Kaiser film holders having negligible prices compared to that (approximately 700 CZK). Below is a table of previously used equipment and price estimates of systems using that equipment. Typical Epson scanners that support scanning film, such as *V600* or *V850* can cost anywhere from 9,000 CZK to 24,000 CZK.

¹⁴<https://www.colorperfect.com/Welcome>

¹⁵<https://www.fotoskoda.cz/>

	Phase One [6]	Nick Carver [11]	Kyle Mcdoughall [12]
Camera	XF	Canon EOS 6D	Fujifilm X-T4
Format	Medium format	Full frame 35 mm	APS C
Resolution	150 MP	20.2 MP	26 MP
Focal length	Depends on lens	100 mm	60 mm
Aperture	f/2.4 - f/3.5	f/11	f/2.8
Body price	1,000,000 CZK	16,000 CZK (discontinued)	50,000 CZK
Full equipment	1,500,000+ CZK	40,000 CZK	80,000 CZK

1.6 Macro photography

Sources for all the information in this subsection are [18] and [19]. Macro photography refers to photographing objects to appear same size or larger than they are in real life, i.e., their projected size on the image sensor (or film) is identical or bigger than their physical size. The common way to represent the enlargement is the *reproduction ratio*, sometimes called *magnification ratio*. A ratio of 1:1 means the photographed object's size is the same as the sensor sees it, that is the preferred ratio for photographing 35mm film with a full frame 35mm sensor.

Using ordinary lens, macro photography would mean bringing the object near the camera, but it may be extremely difficult or impossible to obtain acceptable focus with the photographed object that close to the lens. This leads to the need for specialized equipment (extension rings, macro lens and reverse lens mount) or other methods, such as using a smaller sensor.

*Extension rings*¹⁶ themselves contain no optical elements; they simply move the lens further away from the sensor. Using a combination of extension rings, we can obtain the desired magnification ratio. The lens loses the ability to focus on infinity but can now focus on closer objects instead. One of the downsides of extension rings is that their use negatively impacts the amount of light reaching the sensor, requiring exposure compensation. If the camera is stationary, this dimming is straightforwardly countered by increasing the exposure time. Another downside to extension rings is that the lens will likely exhibit more perceptible optical aberrations, e.g., *distortion*, *chromatic aberration*, or *spherical aberration*, because the lens itself was not designed to focus on such close distances. Yet another problem with cheaper extension rings that lack electrical contacts is that we can't alter the f-number (aperture) and the camera can't automatically adjust focus. Using a *large f-number* is advised to achieve large depth of field, which gets shallower the closer the photographed object is to the lens. With insufficient f-number at such extreme distances, even the slightest misalignment of the sensor plane with the film plane means the camera can't focus on the entirety of the film. Large f-number also aids in minimizing CA, which is very perceptible in the test images taken with $f/2.4$. Example of extension rings that was used in this work is in figure 1.6.1. More details about used equipment is found in section 6.2.

¹⁶<https://www.fotoskoda.cz/mezikrouzky/>



Figure 1.6.1: JJC extension rings for Nikon used in this work.

Using *true macro lens* eliminates the need for additional exposure that is needed with extension rings. Aperture control and autofocus are typically always present, and the lenses are manufactured with CA in mind. They tend to be expensive, however. Phase One *iXG* and *iXH* do not use macro lenses, but come with extension rings, which shows that using calibrated for the lens is sufficient. An example of macro lens is on figure 1.6.2, with details about it in section 6.2.



Figure 1.6.2: True macro lens for Canon used in this work.

“Macro” photography can also be done using a *smaller sensor*, since a 24mm sensor does not need a reproduction ratio of 1:1 to photograph a 35mm object, nor does it need the object to be that close to the lens. Smaller sensors also exhibit a wider depth of field at the same focus distance. All those benefits come at the cost, however, which is higher concentration of electronic elements on the sensor, leading to increased noise. *35-mm equivalent magnification ratio* is used to determine the true reproduction ratio, which considers the smaller size of the sensor.

2 Film density

Film's properties are often given in *optical density*, a logarithmic scale, which better correlates with our perception of light than the linear *transmission* (for that reason, images are gamma encoded, as mentioned in 1.4.1). This section goes over the definition of density, methods and necessary procedures for measuring density and existing methods of linear density encoding (logarithmic encoding, mentioned in 1.4.2). Finally, I will propose a digital printing method that will use aforementioned logarithmic encoding.

2.1 Definition of density

Film's reaction to exposure is best described using density. *Density* is the decadic logarithm of *opacity*, which is the ratio of transmitted (I_t) to incident (I_i) light [3][20]:

$$\text{Transmittance} = T = \frac{I_t}{I_i} \quad (2.1.1)$$

$$\text{Opacity} = O = \frac{1}{T} = \frac{I_i}{I_t} \quad (2.1.2)$$

$$\text{Density} = D = \log_{10} \frac{I_i}{I_t} = \log_{10} O = -\log_{10} T \quad (2.1.3)$$

The relationship is shown on figure 2.1.1.

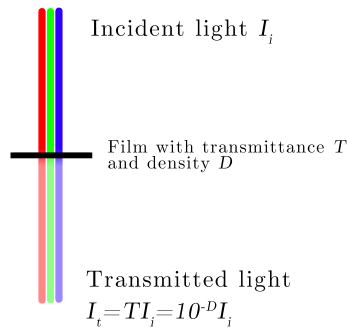


Figure 2.1.1: Effects of transmission and density illustrated on incident and transmitted light. Image by me, based on the formulas above.

In some sources, optical density is also called absorbance or decadic absorbance. Since it is a product of a logarithm, it has no unit. In the case of negative film, the density increases with exposure to light, in the case of reversal film, it decreases with exposure. It is intuitive to understand that while opacity and transmittance are multiplicative, density is additive, since it is a logarithm of those.

$$\log_{10}(O_1 \cdot O_2) = \log_{10} O_1 + \log_{10} O_2 = D_1 + D_2 \quad (2.1.4)$$

2.2 Characteristic curve

The way film responds to exposure is determined by its *characteristic curve* (sensitometric curve, D-LogE curve). This curve has approximately a linear shape when the exposure axis is *logarithmic* (unlike digital photovoltaic sensors, which register light *linearly*). The slope of the linear region is sometimes called *gamma* (this gamma relates to film, it is not to be confused with gamma encoding)

$$\gamma_{film} = \frac{\Delta D_{lin}}{\Delta \log_{10} E_{lin}} \quad (2.2.1)$$

The bottom non-linear region is often called as the *toe*, while the non-linear top region is called the *shoulder*. In color film, the separate layers have separate characteristic curves. The explanations for toe, shoulder and gamma are illustrated on 2.2.1, characteristic curves of real films are shown on 2.2.2.

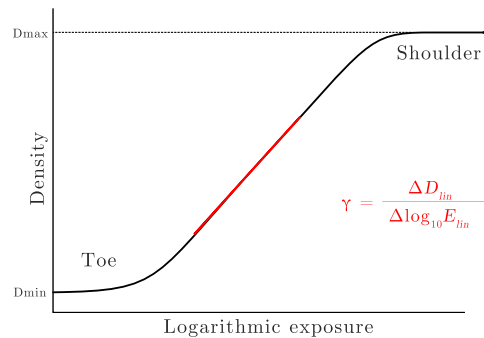


Figure 2.2.1: Illustration of the *toe*, *shoulder* and *gamma* on a characteristic curve of an abstract negative film.

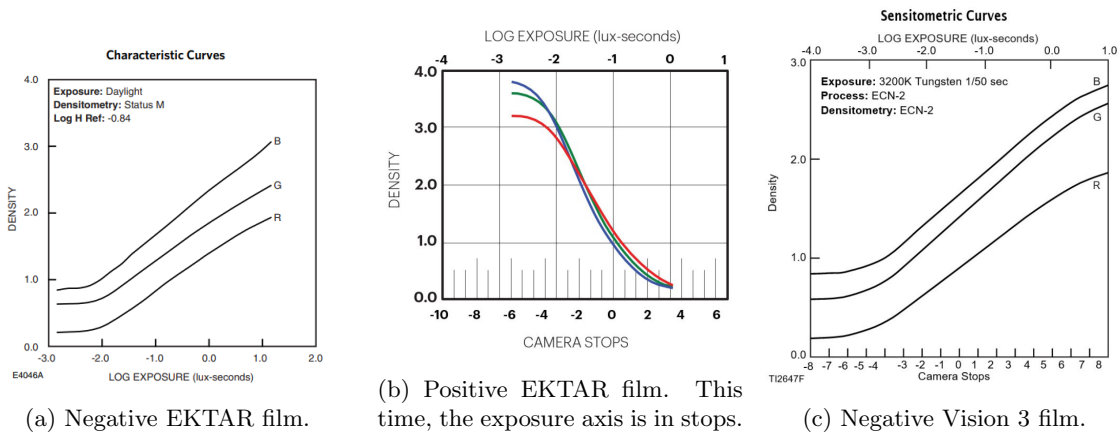


Figure 2.2.2: Characteristic curves of different KODAK films. All images from Kodak, respectively [21], [22] and [23].

The description/units for exposure axis are typically $\text{lx} \cdot \text{s}$, stops, Log. Exposure or EVs. Log. Exposure uses a logarithm with a base of 10, while stops and EVs use a logarithm with a base of 2.

Density range and gamma vary on the type of the film stock and its purpose, for example the *OCN* (original camera negative) is not designed to be viewed by the human eye and typically has a density range around 2 with a gamma of 0.6, while the print stock, meant for screening, uses virtually all 4 stops and has a gamma of 3 [8][3].

2.3 Spectral conditions for color film

Density measurements of color film involve specifying *spectral conditions* of the measuring setup, that is, a color density measuring device can only be called calibrated if we define in the spectrum what those colors passing through the film material are.

2.3.1 Spectral response

A chapter in the book *Digital Color Management* [24] states that scanning densities are determined by effective spectral responsivities:

$$ESR(\lambda) = S(\lambda)M(\lambda)L(\lambda)F(\lambda)SS(\lambda) \quad (2.3.1)$$

where

ESR	effective spetcal responsivity
S	spectral power distribution of the light source
M	spectral reflectance of the mirror
L	spectral transmittance of the lens
SS	spectral sensitivity of the sensor

I did not find another source that would mention *all* of those variables. According to [20] and [8], spectral response is the product of scanning sensor sensitivity and spectral power distribution

of the light source at the same wavelength (i.e. only $ESR(\lambda) = S(\lambda)SS(\lambda)$), which suggests that M and L parameters are negligible or included in SS . Spectral response is calculated and graphed for each spectral sensitivity (R, G, B) separately 2.3.1. This response of the scanning system produces "the net spectral response of an "open gate" or a reading of a perfectly clear material" [20]. It's important to note that when working with spectral responsivities, the values are often normalized to 1 and lack units. It is the position in the spectrum that matters most.

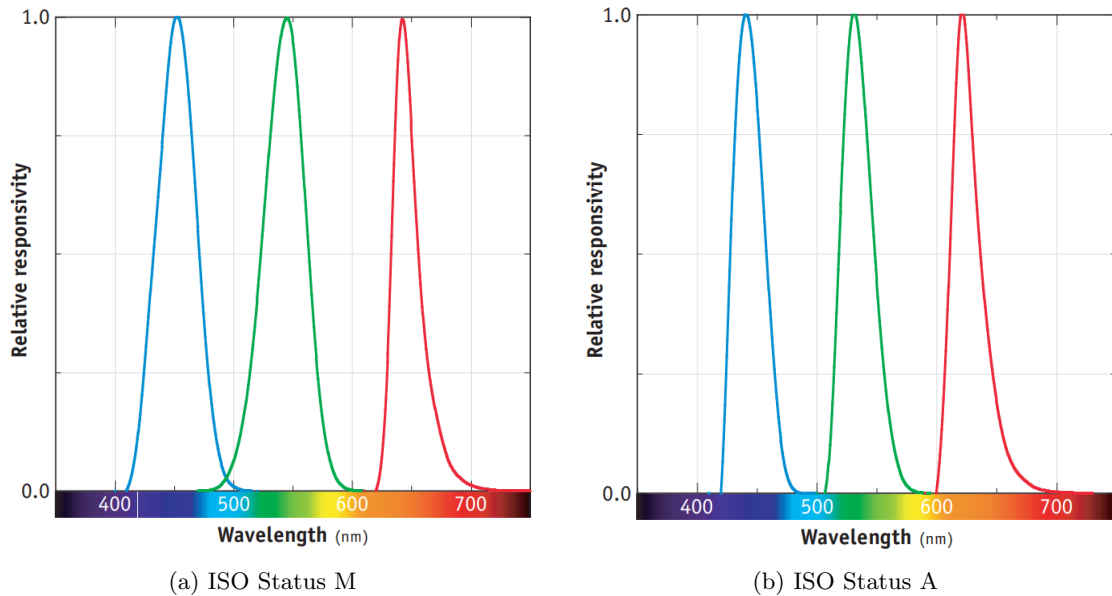


Figure 2.3.1: Process control spectral responses. Image courtesy of [1].

2.3.2 Color separation

Sources [25] and [26] use the term *color separation*, which is tied to side absorption - when two or more dyes absorb the same wavelength, or a digital device captures and writes the same wavelength into 2 color channels, as shown on 2.3.2. Negative films are known to use masking to minimize this unwanted absorption since the 1950s, introducing an orange tint [3]. Since we cannot physically separate individual layers of the film, there is no telling which layer caused the density to increase in regions with side absorption. In practice it means density of the green (or magenta) layer will be partially included in the red (or cyan) channel during scanning. High color separation means the spectral bands scanning the different colors do not overlap and avoid side absorption regions. In return, the individual RGB components of a digital image will contain separate data about red, green and blue densities. Effective spectral responsivities have 3 separate bands in the spectrum for each color, with minimal overlapping. This separation can be achieved multiple ways, for instance by using 3 separate color channels for illumination instead of simply white. The comparison between scanning using white and monochrome illumination is shown on 2.3.3. As the source [25] says, the image captured with narrow band illumination contains more vivid colors and "no amount of processing would retrieve those colors from the image captured with white light and color sensor."

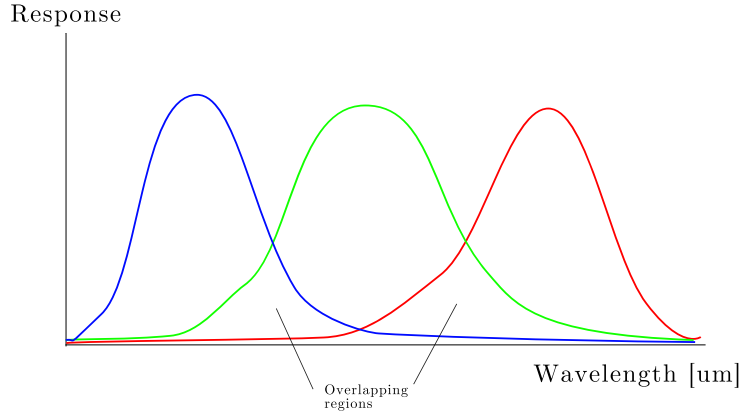


Figure 2.3.2: Spectral response with overlapping side absorption. Image made by me, inspired by [25].



Figure 2.3.3: Comparison of film scanned with white/composite lights and color/monochrome sensors. Image taken from [25].

2.3.3 Types of spectral responses

Spectral responses used for process control are *ISO Status M density* and *ISO Status A density* (also referred to as one of the *printing densities*) 2.3.1. Status M was designed to provide analytical densities and layer-by-layer information most useful for "monitoring film manufacturing and chemical process control" [1]. *Printing densities*, on the other hand, generally try to approximate how the exposed negative will be perceived by the print stock. There is no one standardization when it comes to printing densities, however.

Apart from Status A, numerous further spectral conditions have been developed to describe printing densities, for example [1]: *Cineon printing density* (spectral conditions for the Cineon density were never made public, which resulted in inconsistencies when producing "Cineon" scans

of the same negative when performed by different vendors and facilities), conditions defined by *SMPTE RP-180* and the newer *Academy printing density*'s spectral conditions.

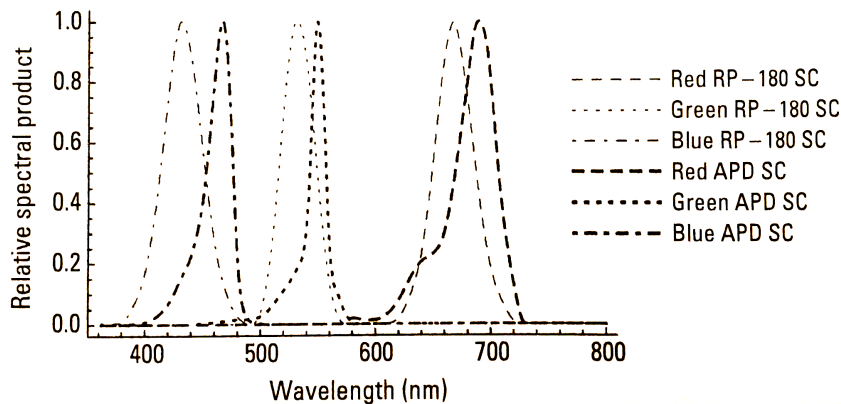


Figure 2.3.4: SMPTE RP-180 and newer Academy Printing Density - spectral conditions. Taken from [1].

The limitation is that in many cases we do not have the option to design scanner fully mimicking the printing process, but instead, we are constrained by existing scanning systems [8] [20]. These systems have to be calibrated by other means to achieve acceptable spectral responses. Furthermore, scanning devices like Cineon and certain ARRISCAN models use additional transformations after scanning to achieve desired look. Cineon utilises 3 by 3 matrices[20], while some ARRISCAN devices also employ transformations after scanning, to approximate the stock as if it were to be scanned by a Status M/printing density device, e.g., [8] a scanner was calibrated as a Status M device, then approximated other printing density by raising the red gamma. The difference between Status M and Status A responses for red is apparent on ARRI's website [27].

Printing densities are used to reproduce how print stock "sees" the negative during the printing process and references [8] and [20] are intended for the digital intermediate process, which is typically performed to digitize film stock for digital post-production purposes, not to digitize archive film material. The vast amount of spectral conditions go to show there is no one right spectral condition to measure density using an imaging chip. Furthermore, the DIASTOR study (focused on dedicated motion picture film scanners, described in section 2.6) has no mention of Status M, A or any densitometry at all [25].

2.4 Spectral conditions for monochrome film

Monochrome film or black and white film is typically sensitive to broader spectrum of light than individual color-sensitive layers of color film and thus does not require precise color separation. Monochrome film is usually divided into 2 categories - *panchromatic* and *orthochromatic*. Panchromatic film absorbs all red, green and blue wavelengths, while orthochromatic film is insensitive to red and sometimes green color. This does not extend to scanning an already developed film,

however it might be optimal to adjust the spectral response in a way that minimal white balance correction is done digitally.

2.5 Densitometer

Densitometer is a device where the film material is placed between light source and photovoltaic cells to directly determine its density. Outside medicine, this method is used mainly for determining the appropriate printing paper by measuring color saturation of the film. It's useful for accurately determining density of a spot and therefore is crucial for supplying data about a calibration sheet that can be used for measuring OECF (Opto-electronic conversion function), but a densitometer can not be used for scanning full images. An example would be the SpecTD¹⁷, which uses tungsten halogen light source and can scan in most spectral conditions described above.

2.6 Dedicated motion picture scanners

Motion picture film scanners are devices specifically designed to scan motion picture film stock. Comparison of 8 different scanners and their parameters was done in the *DIASTOR* project [25]. Examining dedicated motion picture film scanners is useful because it also is a system with a digital sensor and illumination source. *Arriscan 4K* was the only scanner using CMOS sensor, however, while the remaining 7 use a CCD. Charged couple device technology is rarely used in DSLRs.

2.6.1 Illumination source

Illumination sources can be single or composite light sources. *Composite lights* allow adjusting RGB color channels independently or exposing with each color individually, which can be seen in [28]. One scanner offered white light source in addition to adjustable RGB one. Composite lights are an advantage, especially in case of masked negative film (with orange tint), since adjusting white balance can be done directly during scanning, not during color correction. According to [25], if adjusting white balance was done during color correction, the scanning system would "not be taking full advantage of the sensor's dynamic range". Altering illumination intensity might have an impact on the calibration.

Composite light sources also allow for better color separation - color separation was done in 5 out of 8 scanners by using composite light with narrow spectral bands. Remaining scanners used color filters for color separation. With regards to DSLRs - while a camera sensor's spectral sensitivity can not be altered, it is theoretically possible to use narrow-band illuminating source and/or color filters to achieve better color separation.

2.6.2 Sensor pattern

It is mentioned that some scanners use a *monochrome sensor* (Phase One advertised it as *achromatic*), while other use a *color sensor*. Monochrome sensors capture each color component separately to merge them later and present a "true RGB" output. Composite light sources and monochrome sensors go hand in hand. Color sensors use various patterns (e.g. the *Bayer pattern*) and interpolation techniques to fill the missing color information in other channels. Monochrome

¹⁷<https://www.vfx-consulting.com/products-specstd.html>

sensors naturally offer truer representation of colors, though it is unclear to what degree that is perceptible.

2.6.3 Dynamic range

ARRISCAN photographs a single slide at 2 different intensities (it's adjusting the illumination intensity) to cover higher dynamic range. Advanced DSLRs often have a built-in function for shooting at different EVs and merging the image using onboard processor. An option to merge images into HDR is also available in software such as Photoshop or Capture One. More information about specific dynamic ranges of devices is found in section 3.1 and section 6.4.

2.7 Encoding density

At this point it is worth mentioning that motion picture film scanners do not measure and encode density absolutely, they measure density relatively, which is referred to as density above base [29] [8], meaning the density of unexposed film D_{min} is subtracted. The reasoning behind encoding density linearly is the same, that we preserve more useful visual information and map a larger dynamic range.

2.7.1 Cineon and DPX

Scanners typically have an option to encode the data linearly or logarithmically. Originally, *Cineon* only allowed to encode the output (.cin) in log, assigning the sensor code values to 10 bit output file value in fashion depicted on 2.7.1 (negative film is also inverted). This in return enables to calculate density from code values, given by this relationship [8]

$$CV = 95 + 500 \cdot D_{min} \tag{2.7.1}$$

$$D_{min} = \frac{CV}{500 - 0.19} \tag{2.7.2}$$

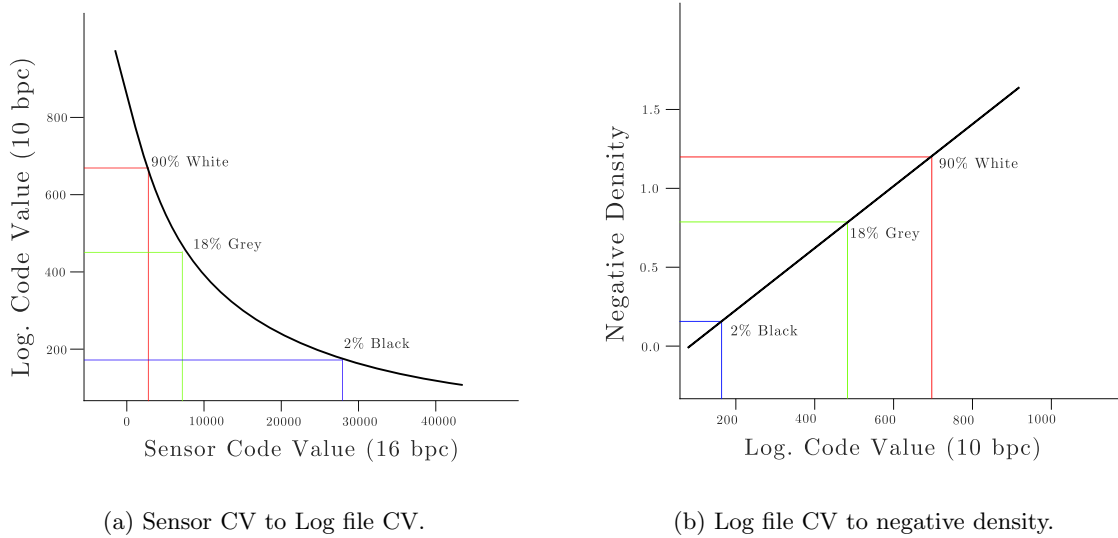


Figure 2.7.1: Cineon's encoding, images inspired by [8].

Several code values are important for Cineon density encoding [29][8]:

CV	
95	D_{min}
180	2% reference black card
470	18% reference grey card
685	90% reference white card

Cineon was designed as a digital intermediate - scanning the original negative as a print stock would "see" it, digitally manipulating the scanned image, then printing the result onto intermediate film for further distribution. Encoding starts at the value 95 to avoid clipping pixels whose densities scanned below average D_{min} [1]. This 10 bpc encoding was designed for older OCN, where $\Delta CV \approx \frac{1}{500} \Delta D$ [1][8] (increase in code value equals 0.002 increase in density) and contemporary scanners offer scanning in 16 bits per channel. This yields the ability to encode the density range of $\frac{1024}{500} \approx 2.048$, with the 95 CVs subtracted, that number becomes 1.86. In order to encompass a higher range of densities in a 10 bpc file, the density resolution can become lower, for instance $\frac{\Delta D}{\Delta CV} = \frac{1}{465}$, which gives us $\frac{1024}{465} \approx 2.2$ or $\frac{1024-95}{465} \approx 2$. A sensor with 14 bit quantization or higher is required to truthfully capture density in $\frac{1}{500}$ increments. The exact transfer characteristic from sensor data to output CVs is described in [25], with the equation being

$$CV_{log} = 95 + 500 \cdot \log_{10} \frac{42000}{i}, \quad (2.7.3)$$

where i is the sensor code value and CV_{log} is the output code value for linear density encoding. DPX files are closely related to Cineon and also permit encoding density values in this manner, whilst offering 8, 10 or 16 bpc. Additionally, DPX files may offer linear output, that is, linear data

from the sensor that does not represent density. Whether or not a DPX file contains information about density is stored in its header [8].

Since we have the option to export lossless RAW linear data from the DSLR's image sensor, it seems possible to calibrate the device so it would encode densities, perhaps using OECF. MATLAB, the tool I'm familiar with, can not handle RAW files, but it accepts TIFF files. The process I will use will be described in 2.7.3 and 7.3 sections.

2.7.2 Log. formats in DSLR

Arri Alexa digital cameras shoot in Log C, which is a direct attempt to match the image produced by a Cineon scanner [10]. Many DSLRs offer shooting in some form of log format defined by the manufacturer. Sony cameras offer *S-Log 2*¹⁸ and *S-Log 3*, Canon offers *Canon Log*¹⁹, Nikon has *N-Log*²⁰. Those may or may not be suitable for encoding density. On the one hand, if they simply logarithmically encode the data and nothing else, then they may offer linear density representation, which can be further examined by finding the OECF. But the exact transfer functions these cameras use are not described anywhere, and if they contain other functions than a logarithm, then it is not likely that they will work. Each format uses different transfer curves varying on manufacturer/model and each requires a different *3D LUT*[30].

2.7.3 Using density information

In most cases, to obtain a presentable picture from digitized film, further steps must be taken after photographing it, especially when dealing with scanned negatives. As was mentioned before in this work, software such as Negative Lab Pro can automatically do most of those steps for us. Another way would be to manually adjust the image using a raster graphics editor. Such process takes time and relies on subjective evaluation of the image. In those graphics editors, if the same set of "subjective" effects is applied on multiple photos, or perhaps folders, there is no guarantee they will look good, or even presentable, because all images occupy different portions of the histogram (and there are three histograms/color components to take care of), meaning some pictures may contain clipping, others will lack or exaggerate contrast, some will have odd color palette. This is exactly where linear encoding of density can be useful - we can use the knowledge of densities to mimic the analog printing process, digitally. That may not guarantee the most subjectively aesthetically pleasing results, but such an approach offers consistency. In section 7.3, in the practical part of this work, I will describe a method I find fitting to perform digital printing.

¹⁸<https://pro.sony/en/CZ/technology/s-log>

¹⁹<https://www.canon.cz/cameras/eos-5d-mark-iv/canon-log-gamma/>

²⁰<https://www.nikonusa.com/en/learn-and-explore/a/tips-and-techniques/what-is-nikon-n-log-and-should-i-use-it-to-record-video.html>

3 HDR

Previous section mentioned the usage of HDR imaging in an ARRI scanner to accommodate for higher dynamic ranges (section 2.6.3). Digital cameras have limited dynamic ranges, ones that might simply not encompass the dynamic range of the scanned film, leading to loss of visual information. Furthermore, if the proposed digital printing method yields a higher dynamic range image than a typical SDR file format can handle, loss of visual information is also inevitable in that case. This section discusses the need for HDR imaging, typical method of acquiring a HDR photograph and methods of storing HDR information.

3.1 Multiple-exposure HDR

Negative film does not have a high range in densities, typically around 2 [3][8], but positive film can achieve a density range nearing 3 or 4. As film fades with age, though, it may lose some dynamic range. If density is the *inverse decadic logarithm of transmission* and transmission describes the percentage of light intensity passing through a medium, then in a scenario where we wish to photograph film with a DSLR, a *change in density by 1* also means a *change of 1 in order of magnitude of light intensity*. Capturing a density range of 4 into a single image then means using a digital sensor that can encompass 4 orders of magnitude of light intensity, at once, into an *SDR image*. Not every camera can do that, for example, in an experiment where OECFs of different cameras were compared [31], one of the cameras cannot even be used above the density range of 2.9. Camera manufacturers and benchmarks do not use OECFs, but they advertise the camera's dynamic range in the number of stops. To roughly estimate the dynamic range of cameras in densities, we need to convert from logarithm with a base of 2 (stops) to a logarithm with a base of 10 (densities):

$$\log_{10} x = \frac{\log_2 x}{\log_2 10} = \frac{\log_2 x}{3.33} \tag{3.1.1}$$

A *Canon 5D Mark IV* can cover *12 stops* of light [32] according to the manufacturer, which equates to *3.6* in density. The site DXOMARK states that the 5D can cover *13.6 stops* [33], which is 4 in density, meaning the lighting conditions must be perfect and there is no headroom. On the same website, *Nikon D700* is said to cover *12.2 stops*, which is a little above than *3.6* in density. While this is only a rough estimate, it points to the potential necessity for acquiring multiple SDR photographs with different exposure settings, so that the SDR photographs can be merged into a HDR image. This approach is often used by film scanners, for instance the Arriscan taking 2 images with different illuminating light intensities. In the case of digital cameras, HDR imaging is done by altering the *exposure time*, since adjusting ISO will also change the amount of noise, while adjusting f-number changes the depth of field and may increase/decrease vignetting. The additional dynamic range is often described in $\pm EV$.

The same problem can be potentially met when exporting digitally printed images, described in previous section. If we take an image of a film with a density of 1.5 and then map that image onto a digital printing paper with 4 densities, the SDR file format will no longer suffice to store that data.

3.2 HDR storage formats

HDR images are stored in formats that tend to be *scene-referred* (as opposed to *output-referred*) and aim to preserve information about real-world luminance. Viewing HDR images directly is problematic and they have to be *tone-mapped* to be displayed on conventional monitors. Description and comparison of different HDR storage methods was done in [34]. Performance of those methods was evaluated based on their ability to preserve brightness, color, as well as their storage costs and efficiency. Table 3.1 portrays the most common lossless formats. The *dynamic range colon* in that table is in orders of magnitude, therefore it is a decadic logarithm, and therefore it can also be seen as *density*.

Extension	Encoding	BPP	bpv	Dynamic range	Relative error (%)
.hdr	RGBE	32	8 + 8 sh. exp.	76 orders	1
.hdr	XYZE	32	8 + 8 sh. exp.	76 orders	1
.tiff	Single precision RGB	96	32	79 orders	0.000,003
.tiff	LogLuv24	24	-	4.8 orders	1.1
.tiff	LogLuv32	32	-	38 orders	0.3
.exr	Half precision RGB	48	16	10.7 orders	0.1

Table 3.1: Most common lossless formats used to store HDR images. Inspired by tables in [34]

3.2.1 Radiance/HDR format

The *Radiance/HDR* format uses RGBE encoding that expands on traditional 24 bpc and provides additional 8 bits to a shared exponent, effectively stretching the amount of code values significantly by allowing a pixel to have certain floating-point benefits. The RGB color space does not allow for negative values, meaning we can't include the entire visible gamut in it. *XYZE* uses the same principle of shared exponent but can encode the entire visible gamut. The source [34] states that relative errors (based on quantization steps) above 5% can be visually perceived and *.hdr*'s relative error of 1% means there is headroom for future manipulation. Both *RGBE* and *XYZE* were written by Greg Ward.

3.2.2 TIFF

.tiff file extension allows for 2 different principles of encoding HDR images, floating point *96 BPP RGB* and *24/32 BPP CIELUV*.

The *96 BPP* and *floating-point representation* means the largest storage costs of all the formats (floating-point generally does not compress well according to the source). It has extremely high accuracy and low relative error to a point that some of it becomes redundant and significant part of the floating-point mantissa is used up by noise, rendering it unsuitable for simple storage purposes. It has uses, however, those being as an intermediate medium and a "gold standard for evaluating different HDR representations".

The *LogLuv24* and *LogLuv32* were also made by Greg Ward, responsible for the Radiance format. They both use a perceptually based *CIELUV color space*, both have a logarithmic luminance L^*

component, but differ in how they cover the gamut. LogLuv24 has 10 bits dedicated to L^* and 14 bits dedicated to a single variable that progressively goes through the u' v' gamut. LogLuv32 has a sign component, 15-bit L^* component and separate 8-bit groups dedicated to u' and v' components. That leaves LogLuv24 with 1.1% relative error and LogLuv32 with a 0.3% relative error.

3.2.3 OpenEXR

EXR was developed by ILM and is nowadays the industry standard for handling and exchanging HDR visual effects shots [1]. It is also an ACES (Academy color encoding system)²¹ compliant format. EXR supports 32 bpc integer and 32 bpc floating-point as well, but those are not as well documented and supported as the half-precision 16 bpc floating point for HDR purposes. The 10.7 orders of magnitude with quantization step size less than 0.1% over most of the range provide enough headroom for manipulation in the future. On each color channel, 1 bit is assigned to the sign, 5 to the exponent and 10 to mantissa.

3.2.4 Comparison of formats

Comparison was done as a part of the book [34] by using 34 test images. One of those utilizes all the gamut and luminance range across 8 orders of magnitude, from 0.01 to 1,000,000 $\frac{\text{cd}}{\text{m}^2}$, as shown on figure 3.2.1. 32 bpc .tiff file was used as the reference due to the format's low quantization step and highest bit depth. It was then encoded into the tested format and decoded back into 32-bit TIFF, which could then be compared using the CIE ΔE^* 1994 formula 3.2.2. An delta larger than 2 is "potentially visible" and above 5 is "evident". It would not make sense to directly compare the entire test images, because humans aren't able to view the entire dynamic range at once. To simulate the human eye accommodating for a certain range, a radius of 50 pixels was chosen around the measured one and the brightest pixel in that area was chosen as the reference. Full color gamut is crucial for color film preservation, and a dynamic range of at least 4 orders of magnitude is crucial for all operations involving film scanning.

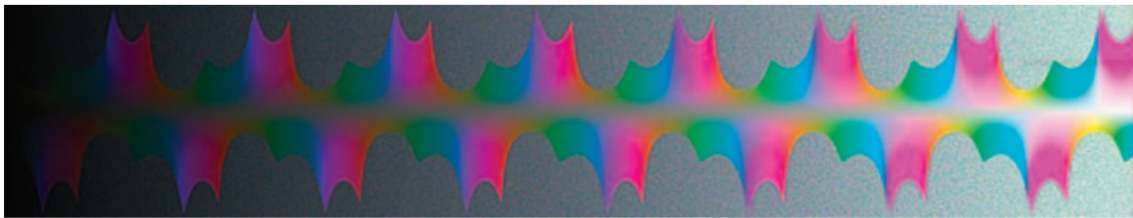


Figure 3.2.1: The test pattern spanning 8 densities and covering all the visible gamut. Image courtesy of [34].

²¹<https://www.oscars.org/science-technology/sci-tech-projects/aces>

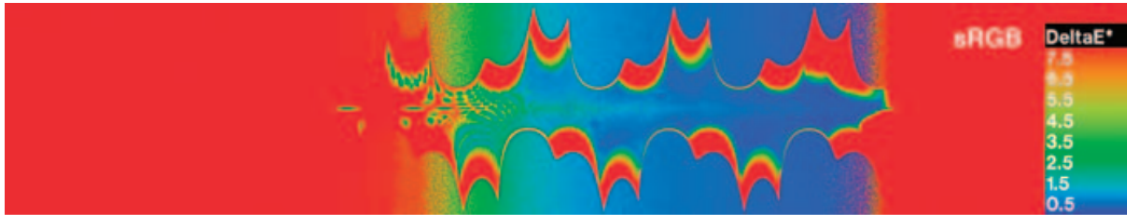


Figure 3.2.2: sRGB’s performance in the test, as well as a color indicator for CIE ΔE^* 1994. Image courtesy of [34].



Figure 3.2.3: Performance of XYZE, LogLuv32 and OpenEXR. All cover the luminance range and gamut. Image courtesy of [34].

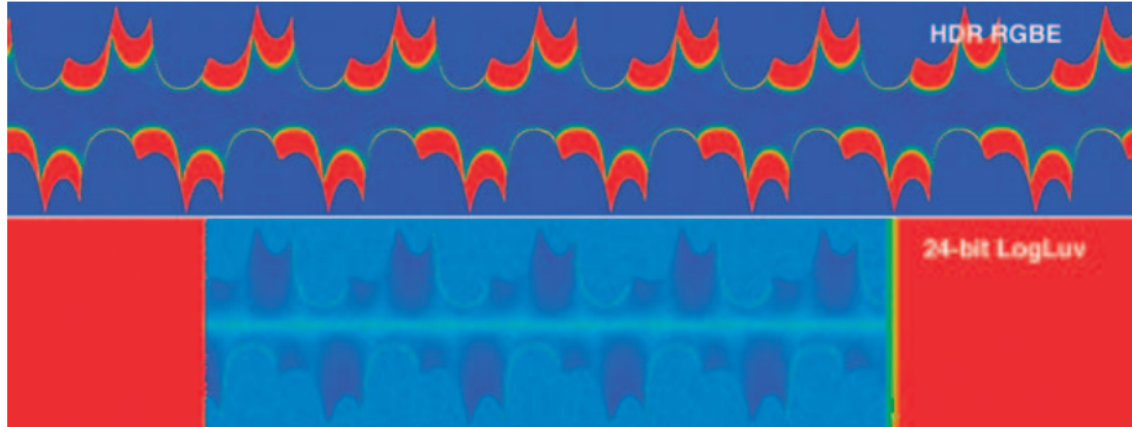


Figure 3.2.4: Performance of LogLuv23 and RGBE. They lack either in dynamic range or color accuracy. [34]

Of the HDR formats stated above, only Radiance XYZE, LogLuv32, 32 bpc TIFF and 16 bpc EXR can cover the *entire gamut* and *full range of luminance values*. LogLuv24 covers the entire gamut but spans only 4.8 orders of magnitude when it comes to luminance. That is, according to the source [34], enough for applications that only need reproducing simultaneous range which humans can adapt to, among those applications are “historical reasons”. Similarly, Radiance RGBE easily spanned the entire dynamic range, but could not achieve highly saturated colors, which is the reason Radiance XYZE was written.

When it came to storage performance, the encoding/decoding speed does not typically matter with still images, however size efficiency does. 32 bpc TIFF is entirely out of the question, but of those other formats that can reproduce the test pattern faithfully, LogLuv32 was the most efficient, with the average value of approximately. 2.4 megabytes per megapixel. All three had average values spanning from 2.4 to 3 megabytes per megapixel, with EXR having the highest variance due to some files having above 4 megabytes per megapixel.

Single precision *32 bpc floating point TIFF* is the resulting intermediate format of most HDR merging software tools, including MATLAB’s *makehdr*, so I deemed it most fit to be used for calculations in this work. For storage purposes, it’s best to use a widespread format that is supported by most software, can encode the desired range of densities ($D = 4$) and covers the visible gamut. LogLuv is not a commonly occurring format in commercial software, as it requires the LibTIFF library or other plugins to operate. RGBE causes loss of color information. Therefore, for storing and interchanging scene referred HDR scans of positive film and photographic paper, it’s advisable to use the *XYZE* or *OpenEXR* format.

4 Optical Aberrations

Compared to a flatbed or drum scanner, DSLR often has a higher number of optical elements, and its sensor is not at all times at a fixed distance from the photographed object, which may result in more perceptible *optical aberrations*. This section covers the most perceptible aberrations and other artifacts that may be encountered during digitization of film using a DSLR, either caused by DSLR itself or other factors.

4.1 Distortion

This type of optical aberration is most noticeable in *variable-zoom lens* with while using the *extreme high and low focal lengths* [2]. While prime lenses are less prone to this effect, wide-angle and telephoto prime lenses can still have perceptible levels of distortion. It is in most cases corrected in software (e.g., Adobe Camera Raw) using profiles for the chosen camera and lens. Certain cameras can resolve this internally using their image processor, either directly before writing a RAW file, or after.

4.2 Vignetting

Vignetting may be visually imperceptible at first but poses a major issue in cases where *stitching* may take place, as illustrated on 4.2.1 [35].



Figure 4.2.1: Stitched image exhibiting vignetting. Image courtesy of [35].

There are several types of vignetting: *mechanical*, *pixel*, *optical* and *natural*. As is clear from the charts on 4.2.2, vignetting is always present on a photograph to a certain degree, regardless of the camera settings. Mechanical vignetting is solved by removing objects obstructing the light path, optical vignetting is minimized by increasing the f-number, increasing focal length, and properly adjusting focus [35].

The remaining vignette must be dealt with after a photograph is taken. Not unlike in the case of distortion, software and camera's built-in solutions can be used. Additionally, vignetting can be corrected manually by taking a *flat-field photograph* of the illumination stand and compensating

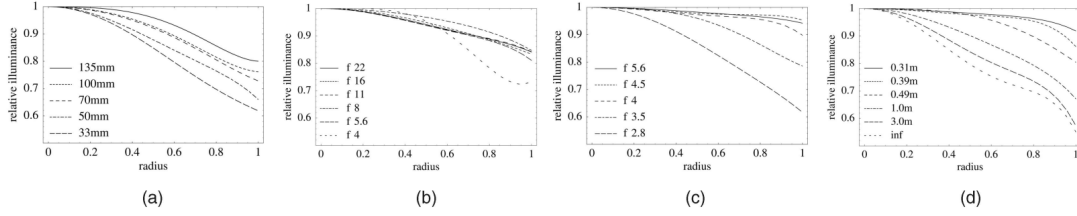


Figure 4.2.2: Vignetting as a function of radius. (a) shows fixed aperture and variable focal lengths, (b) shows varying focal lengths and apertures, (c) shows fixed focal length and varying aperture, (d) shows fixed zoom and aperture, but varying focus distance. Image courtesy of [35].

for the inadequately exposed pixels. This calibration is only valid for that particular combination of focal length, f-number and focus distance, as changing any of those parameters also change the properties of the vignette. Not only does flat-fielding help eliminate vignetting, but it also mitigates the issues coming from *uneven illumination* of the used illuminating table or copy stand. The scanned material itself may contain a vignette that must be preserved, which means flat fielding is preferred to detecting and correcting the vignette using other methods.

I will call the flat-field image \mathbf{F} , raw data of the scanned image \mathbf{R} and the corrected image \mathbf{C} . All of those are matrices whose dimensions depend on image resolution and the amount of color channels (grayscale images have 1 color dimensions, color images typically have 3 color dimensions). [36] and [37] both present a following formula

$$\mathbf{C} = \mathbf{G} \cdot (\mathbf{R} - \mathbf{D}) \quad (4.2.1)$$

\mathbf{D} in this method is a dark frame (dark image), a photograph taken with the camera lens covered with a cap. Subtracting \mathbf{D} from \mathbf{R} is called dark-frame subtraction and is done for de-noising purposes. To account for statistics, multiple photos of both flat field image \mathbf{F} and dark image \mathbf{D} may be taken and merged. The matrix \mathbf{G} (gain) is defined as

$$\text{mean}(\mathbf{F}) - \text{mean}(\mathbf{D}) = (\mathbf{F} - \mathbf{D}) \cdot \mathbf{G} \quad (4.2.2)$$

$$\mathbf{G} = \frac{\text{mean}(\mathbf{F}) - \text{mean}(\mathbf{D})}{\mathbf{F} - \mathbf{D}} \quad (4.2.3)$$

The *mean* operator simply takes the mean value of all the elements in the matrix. The full process is illustrated on a block diagram in figure 4.2.3.

A paper about vignettes in hyperspectral imaging [38] suggests the same formula written using division

$$\mathbf{C} = \frac{\mathbf{R} - \mathbf{D}}{\mathbf{F}}. \quad (4.2.4)$$

While obtaining this flat field matrix \mathbf{F} took additional steps in that article, all the sources show that FFC involves dividing \mathbf{R} by \mathbf{F} . Sometimes we may omit the \mathbf{D} matrix because it is unknown whether the camera performs dark frame subtraction itself, and low ISO setting should

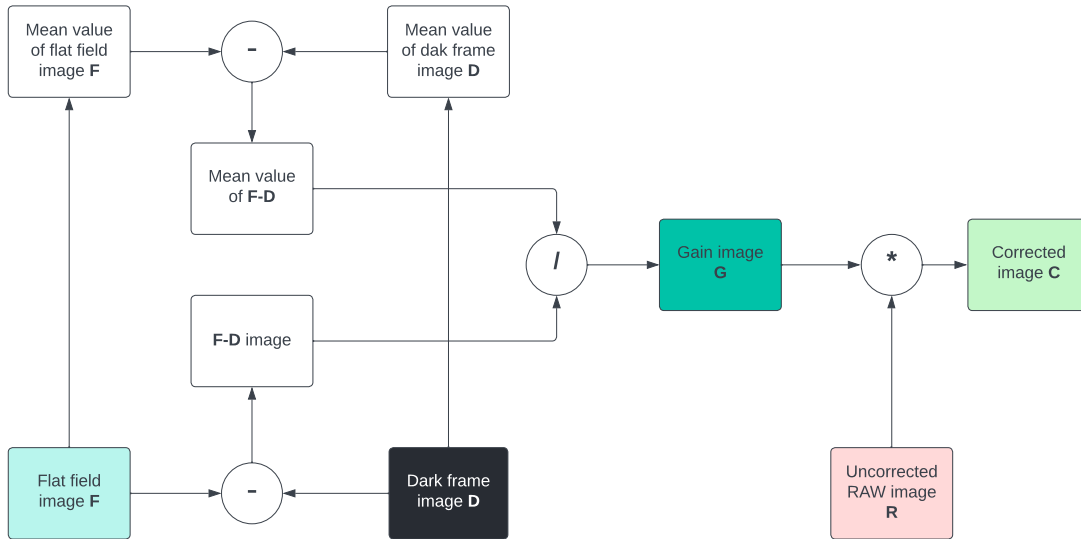


Figure 4.2.3: Flowchart of flat field correction.

yield minimal noise. The full \mathbf{G} matrix then fully takes into consideration the average luminance value of the flat-field image. If we only divide \mathbf{R} by \mathbf{F} , the resulting \mathbf{C} might lose information about absolute luminance, e.g., on a normalized scale, $0.2/0.4$ yields the same result as $0.4/0.8$, but if both pixels are from the same image and same place, we wouldn't know if one of them was originally brighter than the other. Since the *mean* operation is a linear one, exposure time does not matter, because if the image is twice as bright, it will equally affect both the numerator and denominator of \mathbf{G} . Practically, it results in us not needing to use the same exposure time for the raw image \mathbf{R} and flat field image \mathbf{F} . Instead, we must ensure that no values in \mathbf{F} are clipping.

4.3 Chromatic aberration

Chromatic aberration is caused by varying wavelengths having different refraction indexes inside the optics. *Lateral CA*, when all wavelengths of a light ray are on the focus plane, but hitting different parts of the sensor, may be corrected by the image processor or software tools. Correcting lateral CA digitally means *rescaling* individual color layers of the image, possibly leading to loss in resolution. I have not found any studies describing to what degree this is perceptible, but to minimize this effect before a photograph is taken, it is advised to stop down the aperture and not use extreme focal lengths available on camera's lens [2].

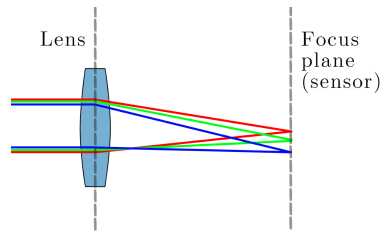


Figure 4.3.1: Lateral chromatic aberration, image inspired by [39].

Longitudinal CA occurs due to the optics' inability to concentrate all wavelengths on the same focus plane. Since information about certain color components is irrecoverably lost due to insufficient focus, longitudinal CA is much harder to correct digitally. It is advised to use optics which compensate for this behavior in the first place [2].

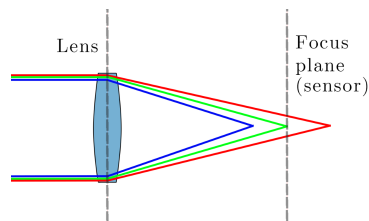


Figure 4.3.2: Longitudinal chromatic aberration, image inspired by [39].

Based on the amount of CA reduction, lenses can be split into *achromat*, *apochromat* and *superachromat* lenses.

4.4 Spherical aberration

SA occurs due to the shape of the optical elements - the angle which a light ray will take after hitting the lens depends on the shape of the lens. These light rays, that may be coming from the same plane, will not all be in focus, causing digitally irrecoverable loss in resolution. *SA* is too corrected by using achromat, apochromat and superachromat lenses, similar to CA. As will be seen on illustrations later, CA and SA pose the biggest problems, as the images are *properly focused only in their center*.

5 OEFC and MTF

This section provides a brief theoretical overview of the performance analysis tools that I will use for evaluating scanning with a DSLR. Those tools are the *Opto-electronic conversion function* and *Modulation transfer function*.

5.1 Opto-electronic conversion function

OEFC [40] describes the relationship between *real-world luminance values* and *CVs* data stored on a RAW file created by an imaging system. Every system has slightly different OEFC, determined mostly by the illumination, DSLR's position and optical path, and DSLR's sensor's capabilities. That goes to show how important it is to maintain parameters across all performed operations once the calibration is complete if we use OEFC for further purposes. Multiple cameras were for example compared in [31] in terms of OEFC. The OEFC allows to calculate the range of densities the system is capable of capturing, with D_{min} being the value camera outputs before clipping and D_{max} being the point at which the signal to noise ratio has a value of 1. To calculate the *SNR*, we also need to calculate *incremental gain* - establishing the dependency between density and increase in CV. The formula for determining incremental gain g_i and SNR are included in the *ISO 14524*²² standard

$$g_i = \frac{1}{2} \cdot \left(\frac{Y_i - Y_{i+1}}{T_i - T_{i+1}} + \frac{Y_{i-1} - Y_i}{T_{i-1} - T_i} \right) \text{ for } i_{max} > i > i_{min}, \quad (5.1.1)$$

$$g_{i_{min}} = \frac{Y_i - Y_{i+1}}{T_i - T_{i+1}}, \quad (5.1.2)$$

$$g_{i_{max}} = \frac{Y_{i-1} - Y_i}{T_{i-1} - T_i}. \quad (5.1.3)$$

$$S/N_i = \frac{T_i g_i}{\sigma_i} \quad (5.1.4)$$

Where Y_i is the weighed luminance CV ($0.2126 \cdot R + 0.7152 \cdot G + 0.0722 \cdot B$), T_i is the transmission of the patch and σ_i is the standart deviation of the patch. OEFC can be measured at multiple stages: on the original SDR image and the HDR image, which is expected to cover larger range of densities.

5.2 Modulation transfer function

Optical transfer function [41] [1] is a complex function that determines how an optical system handles different spatial frequencies. It's obtained by performing a two-dimensional Fourier transform of the point spread function, the system's response to a theoretically infinitely small point in space. Since the OTF is complex, it can be divided into angular and absolute (modulus) components.

$$OTF = MTF \cdot e^{iPTF} \quad (5.2.1)$$

Its angular component (*PTF*) is the phase transfer function, and it describes how the phase shifts with increasing spatial frequency, but it is uncommon to see it used in a measurement. OTF's

²²<https://www.iso.org/standard/43527.html>

absolute component is the modulation transfer function, it represents the imaging system's amplitude as a response to varying spatial frequencies (spatial frequency response). MTF is often, but not always, normalized to its peak value, since it is the relative ratio that interests us.

The units for the horizontal frequency axis may vary. When film was the predominant medium, it made sense to evaluate spatial frequency response in LP/mm (line pairs per millimeter). In the case of flatbed scanners, which also work with physical distance units, LP/mm can be used. However, measuring a MTF involving physical distance units often does not translate well into the digital world, where data is stored in pixels. Units used for digital devices are LW/PH (line width per picture height), LP/PH (line pairs per picture height), LP/pixel (line pairs per pixel, also cycles/pixel) and LW/PH (line width per picture height). 0.5 LP/pixel is the limiting spatial frequency since a single line of pixels can only sample/display one line.

LP/pixel doesn't always provide sufficient information because it does not consider the dimensions of the image. For example, an imaging system that has a horizontal resolution of 320 pixels and whose MTF approaches zero at 0.5 cycles/pixel will contain less detail than an imaging system whose MTF approaches zero at 0.4 cycles/pixel, but it has a horizontal resolution of 2000 pixels. In that situation, it would be appropriate to use LP/PH. We can convert from LP/pixel to LP/PH by multiplying LP/pixel by the number of pixels. If we desire to use LW/PH, we multiply LP/PH by 2, since a pair of lines contains 2 lines.

6 Sample acquisition, digitizing and performance evaluation

The goal of this section is to demonstrate the methods by which acquired and digitized film samples with two DSLRs (*Canon EOS 5D Mark IV*²³ and *Nikon D700*²⁴) and how I used objective metrics to evaluate the performance of those methods, those metrics being *OECF* (Opto-electric conversion function) and *MTF* (Motulation transfer function). Comparison was done in relation to Epson V550 scanner, capable of scanning in transmissive mode²⁵.

6.1 Film samples

In order to perform digitization, I needed 35 mm film samples. I was provided with a *Canon AE-1 Program*²⁶ film camera with manual focus and capability to automatically adjust f-number based on lighting conditions, selected ISO speed and selected shutter speed. The device is shown in figure 6.1.2. For negative film, I chose the *Fomapan 100* 35 mm film²⁷ due to its availability, as well as its advertised low granularity and sharpness. As to reversal film, I chose *Fomapan R100*²⁸, for the same reasons. I selected 4 film samples - a low dynamic range photo of 2 guitars (negative and positive) and a high dynamic range photo of the Prague Castle (negative and positive), shown below in figure 6.1.1



Figure 6.1.1: Film samples used in the practical part of this work, positive and negative images of guitars and Prague Castle. These exact photos were taken with 5D. The bar visible on top of these images is not part of the samples, but it ensured the film is flattened out (no parts are protruding).

²³<https://www.megapixel.cz/canon-eos-5d-mark-iv-telo>

²⁴<https://www.megapixel.cz/nikon-d700>

²⁵<https://www.mall.cz/skenery/epson-perfection-v550-photo>

²⁶https://en.wikipedia.org/wiki/Canon_AE-1_Program

²⁷<https://www.foma.cz/cs/fomapan-100>

²⁸<https://www.foma.cz/cs/fomapan-R-100>



Figure 6.1.2: Canon AE-1 Program film camera and negative grayscale film that I used to take the samples with.

6.2 Digitizing equipment

In three different setups, I used two different full-frame cameras, one is the discontinued *Nikon D700* and the other is the *Canon EOS 5D Mark IV*, which is shown in figures 6.2.1a and 6.2.1b. For macro photography, I outfitted the Nikon with extension rings from JJC²⁹, which when combined, can yield varying magnification ratios. At first, I used a ratio of 1:1.07, but that combination of rings (12 mm+36 mm) did not allow for changing the $f/$ number due to issue with electrical contacts, so it was fixed at $f/2.4$. To address that during the next measurement, I utilized only the 36 mm extension ring, compromising sufficient magnification ratio (it was only 0.86:1) for the ability to change $f/$ number under the premise that it would increase the depth of field and mitigate optical aberrations. The 5D was outfitted with macro lens *Canon MP-E 65mm $f/2.8$ 1-5x Macro Photo* with varying magnification ratio³⁰ of 1:1 to 5:1, and proved to be much better at dealing with optical aberrations. Of course, I only used the 1:1 setting. F-number was varied, I took samples with aperture from $f/2.8$ to $f/16$. All setups used the Manfrotto MICRO 454³¹ as the mount for camera, it allowed for precise control with small increments in 2 axes - an incredibly useful tool, considering that focus in macro photography is achieved by changing the distance to the photographed subject. I judged by eye how focused the scanned material was, by using the maximum zoom in the live view mode of the cameras.

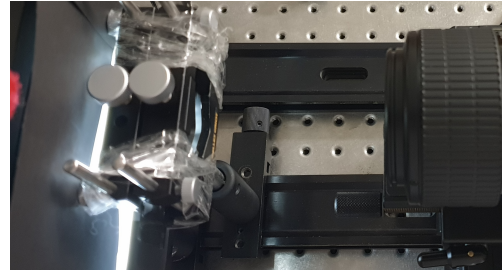
²⁹<https://www.megapixel.cz/jjc-sada-mezikrouzku-12mm-20mm-36mm-pro-nikon>

³⁰<https://www.canon.cz/lenses/mp-e-65mm-f-2-8-1-5x-macro-photo-lens/>

³¹<https://www.megapixel.cz/manfrotto-stativova-desticka-micro-454>



(a) 5D in the 3rd setup mentioned in this section.



(b) 5D in the 3rd setup mentioned in this section, view from above. I aligned the Canon macro lens with film and turned off the ambient light when taking samples, this image only demonstrates the setup.

Figure 6.2.1: Images of setup using *Canon EOS 5D Mark IV*, *Canon MP-E 65mm f/2.8 1-5x Macro Photo lens* and a rail system.

In the first setup with D700, the light source was a fluorescent *Just Normchild Color Match 5000*³². It is slanted, so in order to accommodate for the angle, the camera was stationed on a tripod. This is less than ideal, because the film and sensor plane need to be parallel, and the only way of telling that angle was by eye. Additionally, any vertical movement of the camera had to be done by adjusting the tripod's legs, which almost always resulted in misalignment of the planes. This was solved in the second setup, where I used a small LED panel, *Medalight LP-100*³³. Both the camera and the light source were mounted on a rail system from *Edmund Optics*³⁴, which assured better alignment. The setup with 5D also used this light source and rail system, see figure 6.2.1a. To isolate the camera from unnecessary light (not coming from behind the film), I used black paper, and all the remaining light sources in the room were off. In the second setup with D700, where I taped the film directly to the light panel, I did not figure out how to avoid light spill. That led to decreased dynamic range as seen in figure 6.2.2a – the entire image has a perceptible white cast compared to figure 6.2.2b. The film samples were B&W, so a high CRI of the light sources were not necessary. During the 1st setup with Nikon, I took samples fitting for OECF due to the better light isolation. The 2nd setup with Nikon did not have that light isolation, but keeping the entirety of the scanned material in focus was easier, so from that measurement, I obtained data for MTF. The 3rd setup with Canon allowed for both good OECF and MTF samples. During all measurements, I did not press the shutter button directly, I used either a remote trigger, or a timer, so that the cameras was as stationary as possible. Following is a table (6.1) of specifications and hardware used in the setups, as well as rough price estimates of the equipment used. It's important to remember that the D700 is discontinued, and I took the original price from when the camera was released,

³²https://www.bhphotovideo.com/c/product/187548-REG/Just_10801.12_x.18_Color.html

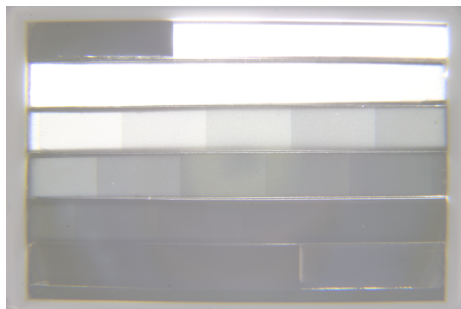
³³<https://www.amazon.com/Medalight-LP-100N-Inches-Ultra-Thin-Negative/dp/B07TYLR7VT>

³⁴<https://www.edmundoptics.com/c/manual-translation-stages-and-slides/>

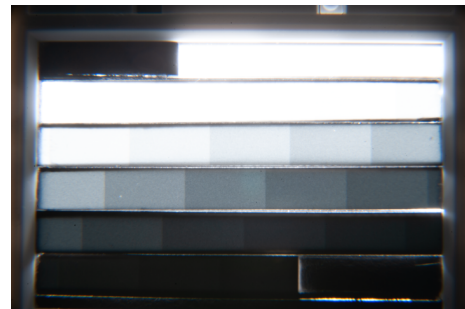
2008.

Setup	1	2	3
Camera	D700	D700	5D Mark IV
Resolution	4276 by 2836 pixels	4276 by 2836 pixels	6720 by 4480 pixels
ISO	200	200	100
Focal length	50 mm	50 mm	65 mm
Macro tool	12 + 36 mm ext. rings	36 mm ext. ring	Macro lens
Magnific. ratio	1.07:1	0.86:1	1:1
F-number	f/2.4	f/8, f/11 and f/16	f/2.8 - f/16
RAW file bit depth	14 bpc	14 bpc	14 bpc
RAW file format	.NEF	.NEF	.CR2
White balance	Auto	Auto	Auto
Light source model	Color Match 5000	LP-100	LP-100
Light type	Fluorescent	LED	LED
Advertised temperature	5000 K	5200 K	5200 K
Estimated total cost (CZK)	78,000	54,000	100,000

Table 6.1: Used hardware and its specifications.



(a) Density calibration sheet with white cast due to light spill, taken with high exposure time. Captured using Nikon D700 and 12 mm + 36 mm extension ring.



(b) Density calibration sheet with better isolation, taken with high exposure time. Captured using Nikon D700 and 12 mm + 36 mm combination of extension rings.

In order to compare the performance of the DSLRs to a different digitizing method, I used a flatbed *Epson Perfection V550* scanner, shown on 6.2.3. I used 16 bpc quantization and TIFF file format as well.



Figure 6.2.3: Epson Perfection V550 scanner, photo courtesy of *Mall.cz*.

I used the RAW .NEF and .CR2 files to generate linear (not gamma encoded) 16 bpc TIFF files and performed tests on those. Conversion was done using the LibRaw library³⁵ that is based on the *dcraw* library³⁶. An example of a system command to convert a RAW photo into 16 bpc linear TIFF would be

```
dcraw_emu.exe -4 -T -Z tif FILENAME.CR2.
```

MATLAB has a function *system* that allows to call operating system's console commands. At no point did I use JPEG or other lossy formats to perform evaluation of OECF and MTF, I used those to export the images for illustration in this work.

³⁵<https://www.libraw.org/about>

³⁶<https://www.dechifro.org/dcraw/>

6.3 Flat-field correction

I implemented a short script in MATLAB (*FFC.m*), based on flowchart shown in figure 6.3.1. Below are images of an *uncorrected flat field image* (figure 6.3.2a) and that FF image *corrected by itself* (figure 6.3.2a). Figure 6.3.3a depicts the *uncorrected OEFC chart image* and figure 6.3.3b shows the *flat field corrected image*. The vignetting present around the edges has disappeared.

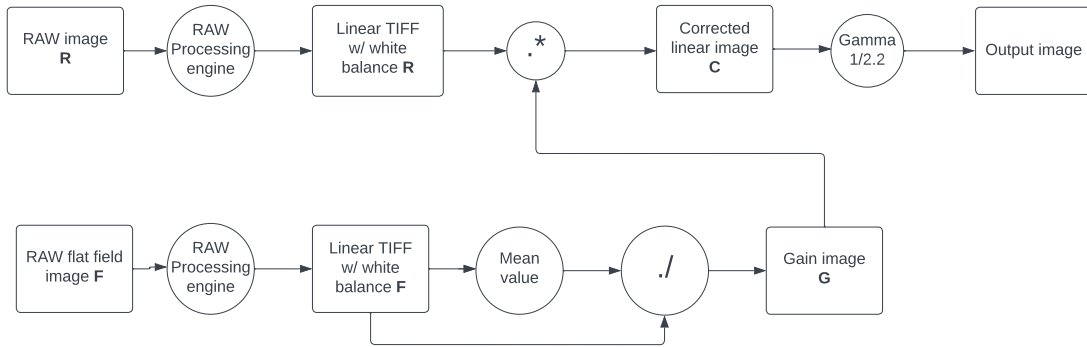
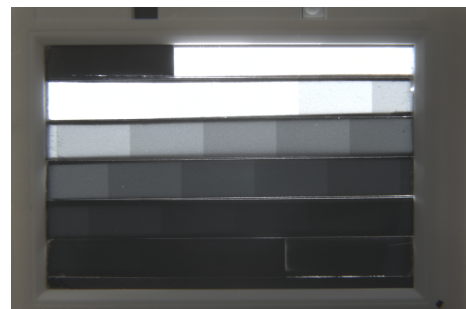
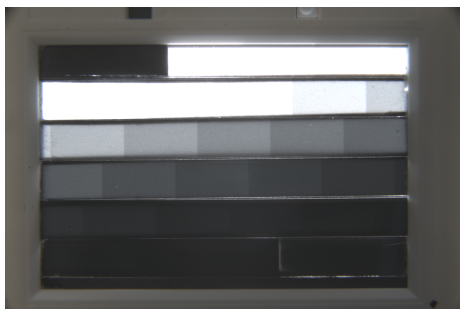
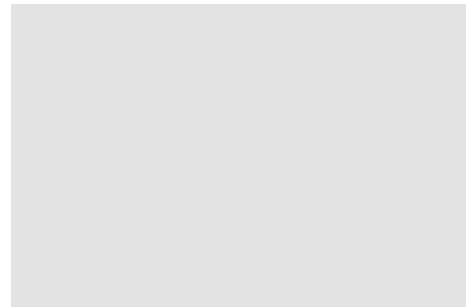


Figure 6.3.1: Flowchart of MATLAB script.



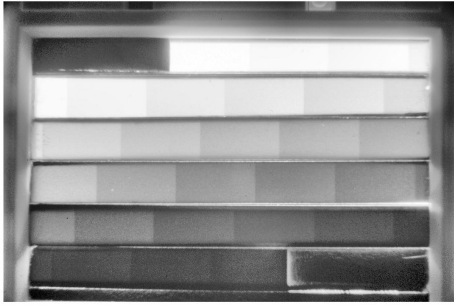
6.4 OECF measurement

To measure OECF (*scripts OECF.m, CalculateIncGain.m*), I used the TS28 density calibration sheet, made by Danes Picta ³⁷. The densities of the calibration chart are below in table 6.2. I implemented two scripts and a function in MATLAB that measure and plot *OECF*, *incremental gain* and *S/N ratio* using a photograph of the density sheet, in accordance with the definitions and formulas described in section 5. The script works by manually selecting a part of an image using the *imcrop* function, storing its average value (average CV) and calculating standard deviation. I did this for SDR and HDR images of D700 and 5D, and the V550 scanner. To combine SDR photos into an HDR one, I used multiple images of the calibration sheet spaced 1 EV apart (7 images for D700, 9 images for 5D), and merged them into a single precision floating point HDR using the MATLAB function *makehdr*. The resulting tone-mapped sheets are in figures 6.4.1a and 6.4.1b, they have been made from a gamma-corrected set of SDR images, because linear images did not yield visually intuitive and pleasing results. As can be seen, all individual patches are discernible, albeit the highest densities at the bottom include visible noise. It is not advised to select the CVs from the tone-mapped image at all, as tone-mapping is local and we can see that patches are not progressively darker. Where possible, I used the tone-mapped HDR images as a reference, to ensure I select the right patches extreme densities. To select the patches for the V550, I had no choice but to adjust my monitor's gamma to see into the patches with higher densities. I entered known values of densities of the patches manually into a vector, and also calculated transmission. The OECF for mentioned devices is in figure 6.4.2, incremental gain and S/N are on chart 6.4.3.

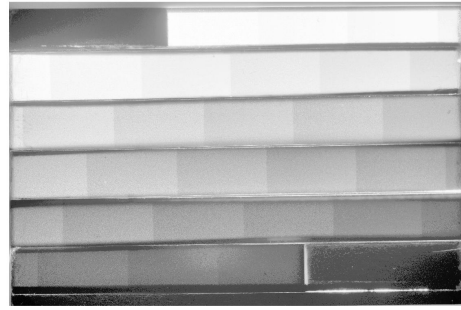
Densities	
0.15	2.22
0.32	2.38
0.46	2.53
0.62	2.68
0.76	2.81
0.9	2.96
1.06	3.12
1.2	3.28
1.34	3.42
1.49	3.56
1.64	3.68
1.79	3.84
1.93	4
2.08	4.17

Table 6.2: Density values of the individual patches, TS28 calibration sheet.

³⁷<https://www.danes-picta.com/>



(a) Tone-mapped HDR image from Nikon D700.



(b) Tone-mapped HDR image from Canon EOS 5D Mark IV.

Figure 6.4.1: Tone-mapped HDR images of the TS28 density calibration sheet from Danes Picta.

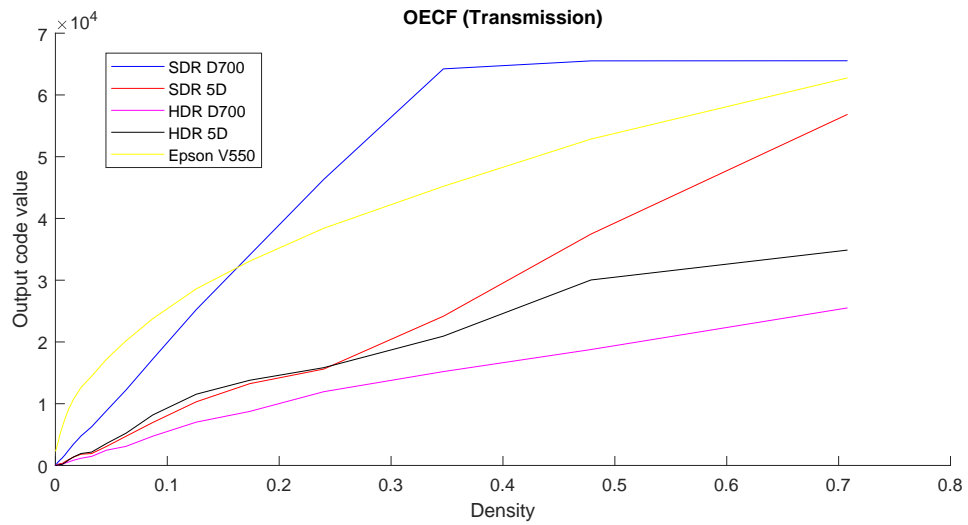
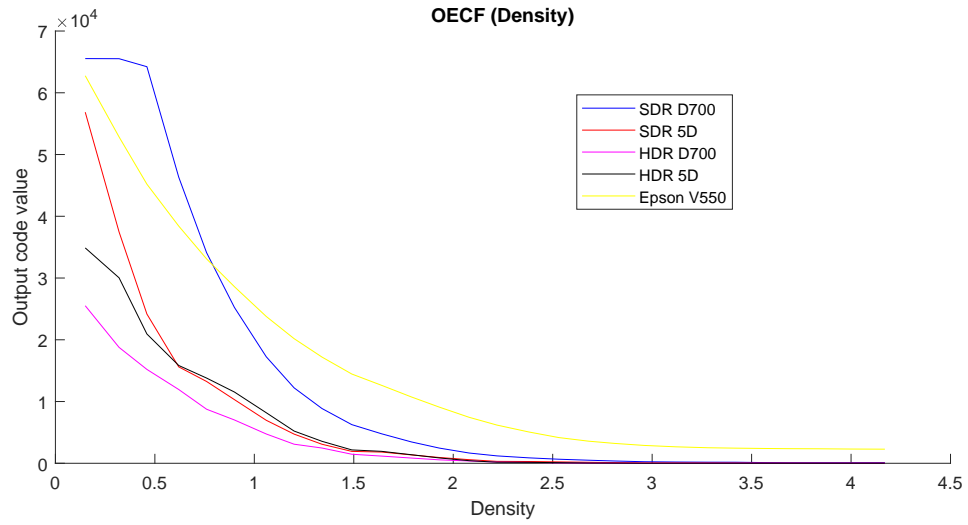


Figure 6.4.2: OECF comparison of D700, 5D and Epson V550.

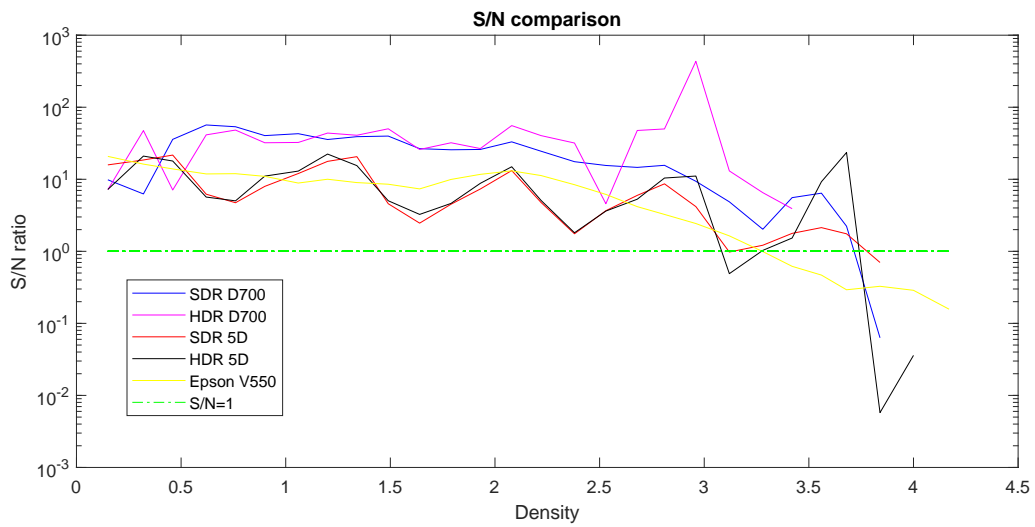
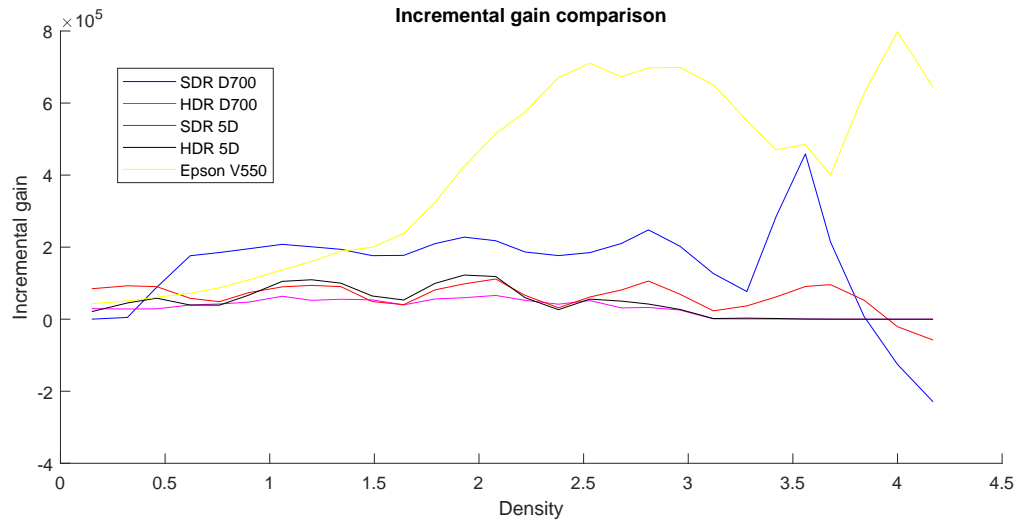


Figure 6.4.3: Incremental gain and S/N comparison of D700, 5D and Epson V550.

While relationship between CVs and transmission is linear for SDR D700, we can see it deviate in the case of 5D - it has a semiperiodic nature, in figure 6.4.3. The period is exactly the amount of patches in a single row, meaning the cause is improper illumination, the left side is brighter than the right side. It makes sense, because the black paper covering the illumination source was **behind** the TSD28, and I may have not noticed that it is obstructing the light on the right. 5D's S/N drops below 1 at 3.12 due to this effect, but then rises above 1 again. This is not due to the camera's limitations, but because of the uneven illumination.

Even though 5D is a newer device, the dynamic ranges of the two DSLRs are comparable, they do not clip in $D = 0.15$, and S/N drops below 1 after $D = 3.68$, leaving a range of **3.53 D**. Besides S/N, I also tried a different, subjective method of evaluating the dynamic range, which is closely tied to logarithmic transformations. If I apply a logarithmic transfer function onto the stored CVs from the devices and then plot the result against densities, the relationship should be linear. If it stops being linear at some points, it is probably caused by the device's limitations. The applied transfer curve along with transformed CVs plotted against densities are below in figure 6.4.4 below. The precise formula is

$$CV_{out} = 13600 \cdot \log_{10}(CV_{in} + 1). \quad (6.4.1)$$

The reasoning behind those exact coefficients is explained later in detail in section 7.1, they ensure that minimal values are clipping and the range of densities fully utilizes the 16-bit space.

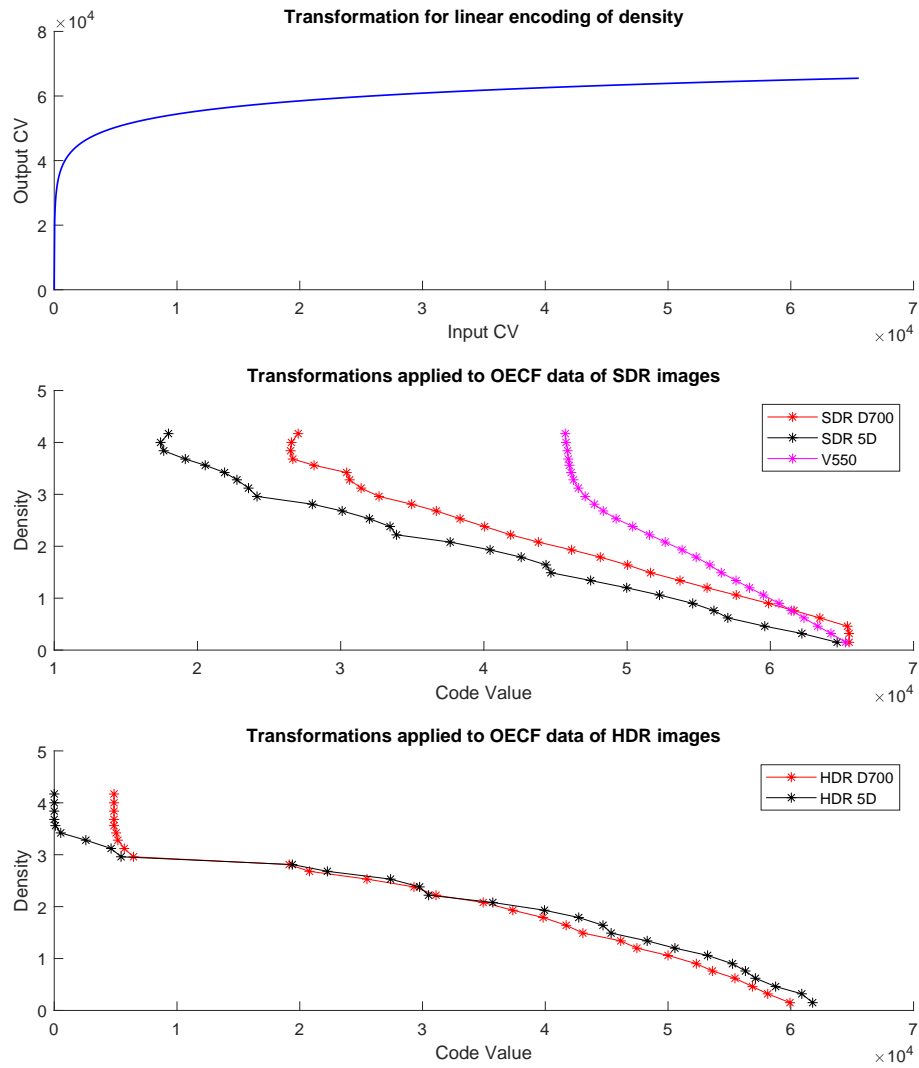


Figure 6.4.4: Logarithmic transfer curve for linear density encoding, as well as that curve applied to measured OECF data shown in previous figures.

Due to imperfections in lighting conditions (light spill) and the HDR merging algorithm, the density relationship for HDR is not perfectly logarithmic, but only approximates that. Similarly, the transmission graph shows that it's not completely linear, either the makehdr algorithm includes an additional transformation in itself, or this is caused by lighting conditions. For D700, the lightest values are not clipping at all, but the moment of S/N dropping below 1 always varied when I selected the patches in MATLAB using the *imcrop* tool. In the figure 6.4.3 above, it is $D = 3.42$, leaving a dynamic range of **3.27 D**. However, during some other *imcrop* selection, max. density was for example $D = 3.68$. The position where I cropped a patch plays a role as well, which should not be the case - it points to light spill. The tone-mapped images show this, the individual patches are not uniform, parts of the patches reflect light more than others. The edges of the sheet are made of white plastic, which reflects some light as well. It might be reasonable to assume that under near-ideal isolation, like the V550 has, we'll be able to encompass the full density range of the sheet with DSLRs. If we judge the dynamic range by the darkest value the D700's HDR version achieves before it clips, then the max. density is $D = 3.56$, with a dynamic range of **3.41 D**, identical to the scanner's.

As to the HDR version coming from 5D, the lowest densities are also not clipping and its S/N falls below 1 at $D = 3.12$, however, then it goes back up above it, meaning it is not a reliable indicator of dynamic range in this case. If we judge the dynamic range by data in figure 6.4.4, then the highest value that is not clipped (in the dark) is $D = 3.68$, leaving a total dynamic range of **3.53 D**, the same as SDR of D700 and 5D.

The output TIFF image of the V550 scanner contains some form of gamma transformation - the transmission chart is not perfectly linear, nor does the scanner make use of the full 16-bit space. The dynamic range of the scanner is **3.41 D**, worse than SDR versions of both D700 and 5D, as well as HDR version of 5D.

I previously assumed that using scans where the lowest densities clip will allow me to have higher S/N in the higher densities, but I was wrong. Using the lowest exposure time yielded the best results, while using a middle exposure photo resulted in a lower dynamic range for SDR, approximately 3.56, same as HDR of D700. There is was advantage to using HDR merging in my work, the dynamic ranges are identical. Perhaps, that is because I have not been able to achieve enough protection from ambient/reflected light for the DSLRs with TSD28, and during high exposure times, the low density patches let too much light through, which in turn gets reflected from the edges of the chart/other objects back onto the dark patches. If the dark patches reflect this light into camera, they render the transmission test useless, because now the chart has reflective properties as well. Deviation of those patches may then rise, lowering the S/N. V550 scans the TSD28 one line at a time, avoiding this overexposure. Perhaps, a better approach in the future might be to photograph individual patches of density, instead of capturing them all in one image.

The dynamic ranges and density extremes are below in table 6.3. Data for HDR was taken using subjective method using log. transformations (darkest patch before clipping, as seen on the left of the figure), since the S/N is not as consistent and varies highly with every iteration of the script (different regions of the patches are selected). 6.4.4

	SDR D700	HDR D700	V550	SDR 5D	HDR 5D
D_{min}	0.15	0.15	0.15	0.15	0.15
D_{max}	3.68	3.56	3.56	3.68	3.68
D_{range}	3.53	3.41	3.41	3.53	3.53

Table 6.3: Density extremes and ranges.

6.5 MTF/SFR measurement

Spatial frequency response can be calculated from either ESF (edge spread function) or a sweep-pattern, such as a sine or square wave with progressively increasing frequency. Square patterns are used more often because they are easier to manufacture. The results of spatial frequency analysis using a square pattern (sometimes called CTF, contrast transfer function) are often better than the ones produced by sine pattern. The relationship is approximately following: $MTF = \frac{CTF \cdot \pi}{4}$ ³⁸. Since using ESF is considered to be more reliable and accurate, I decided to use it for measurements, and use the sweep pattern only for illustrations. I utilized the MATLAB tool *sfrmat4* available from [42], and a 35 mm FSR2 test chart from Danes Picta. This ESF uses the same visual weighing coefficients for RGB to grayscale as for OECF. I discarded the values above 0.5 LP/pixel, as those are aliases.

First, it's important to say that flatbed scanners like V550 do not have one single resolution, they offer scanning in multiple DPI options. I first scanned the FSR2 sheet with multiple DPIs, 600, 1200, 2400, 3200 and 4800. All were in color but 3200, which was scanned in grayscale mode. Results are shown in figure 6.5.1.

³⁸<https://www.sciencedirect.com/topics/engineering/modulation-transfer-function>

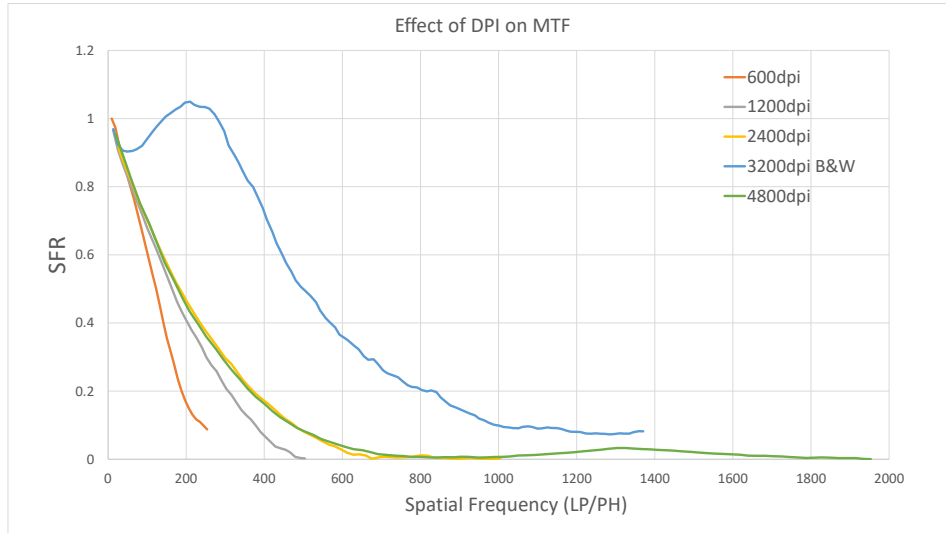
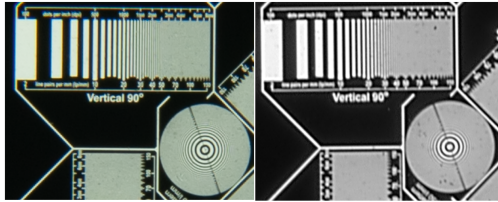
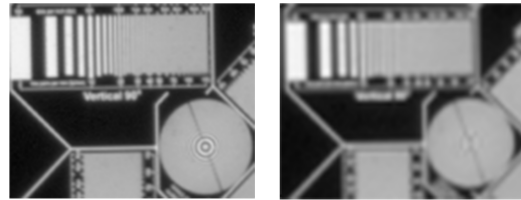
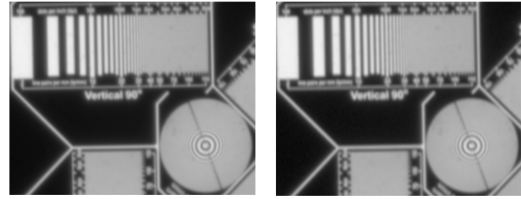


Figure 6.5.1: Scans taken with V550, all in color except for 3200 DPI.

Figures 6.5.2a and 6.5.2b below are provided for subjective evaluation/illustration.



(a) Sweep pattern scanned with D700 and V550 at 3200dpi (B&W)



(b) Sweep pattern scanned using 4800, 2400, 1200 and 600 dpi (left to right, top to bottom), color.

It's evident that grayscale mode is superior to color mode, perhaps it is due to CA, which when converted to grayscale will manifest as blur. Therefore, I evaluated MTF of grayscale only scanning modes, and resulting MTF is shown in figure 6.5.3. Based on that chart, we can see that increasing DPI above 2400 is not necessary and only inflates file sizes. The next question is what f-number do we use to scan with the DSLRs. High f-number allegedly yields *bigger DoF* and mitigates CA and SA. Using 5D, I took images with f-numbers ranging from $f/4$ to $f/16$, MTF is shown in figure 6.5.4.

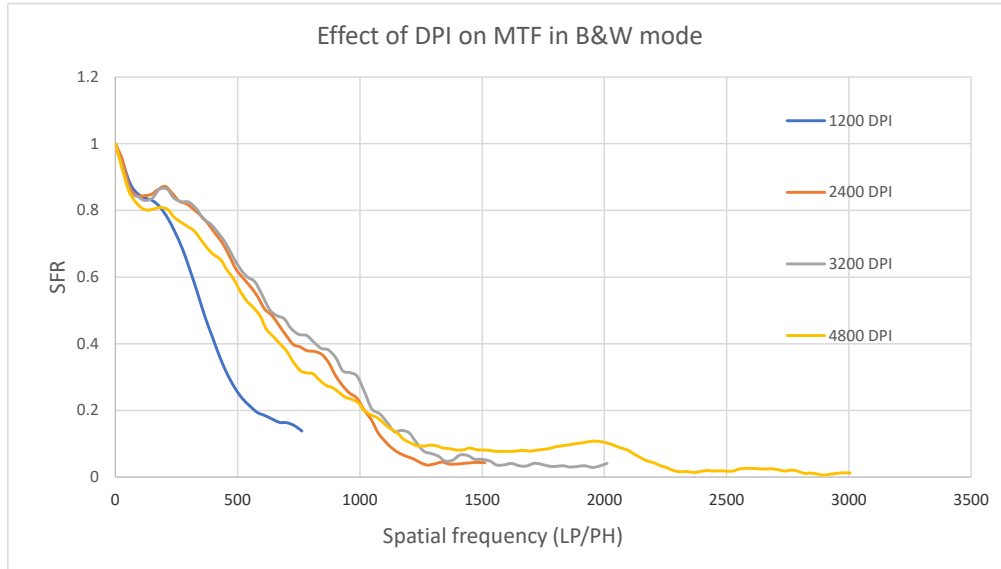


Figure 6.5.3: Effect of DPI on MTF in B&W mode.

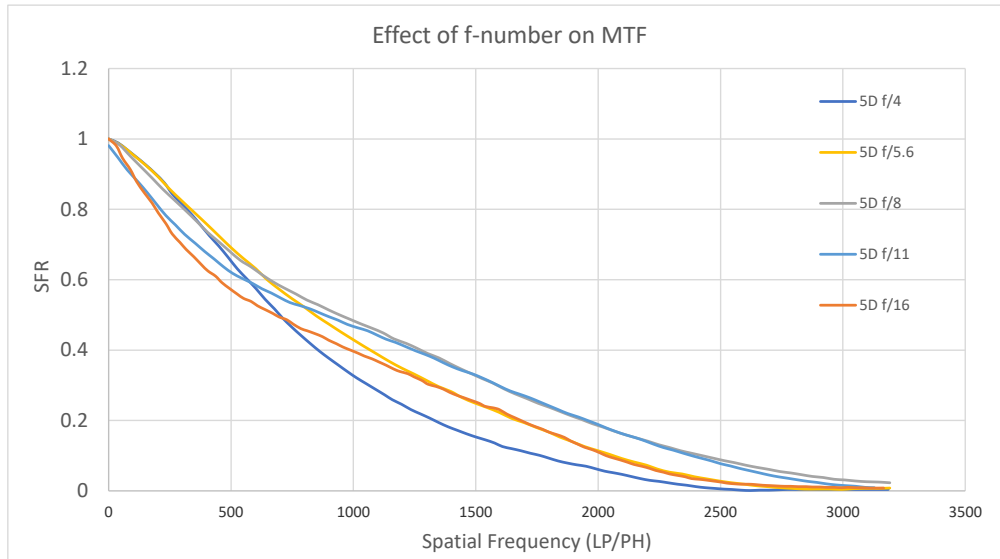


Figure 6.5.4: Effect of f-number on MTF, 5D.

Of all apertures, f/8 and f/11 have the best MTF, with f/8 having a slight edge on the figure above. For 5D, I will use f/8 in comparison. Nikon D700 uses extension rings, and exhibits extreme chromatic aberration near the edges, therefore I used f/16 in MTF comparison of all three devices, shown in figure 6.5.5 in LP/PH and 6.5.6 in LP/mm.

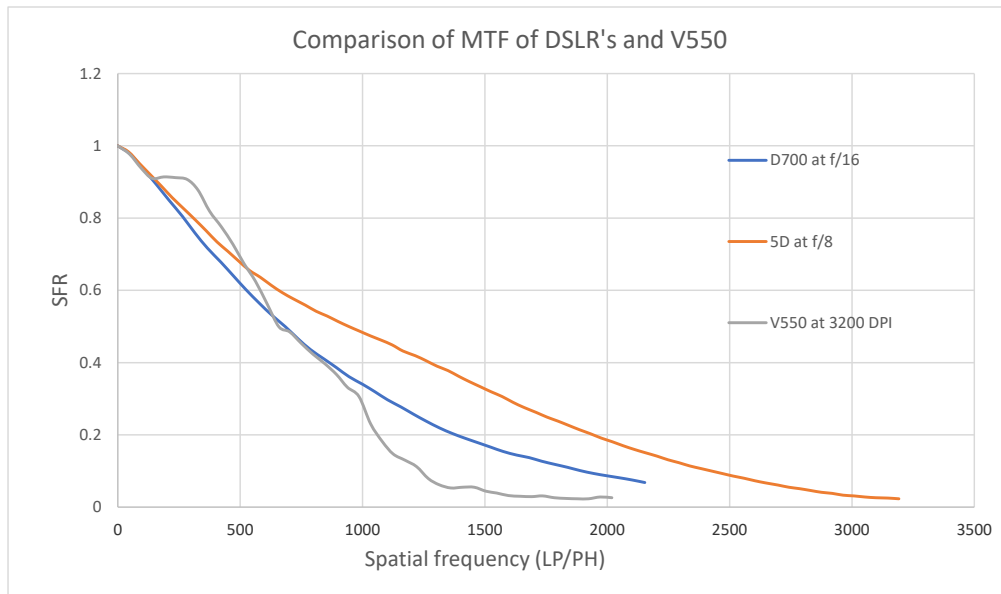


Figure 6.5.5: Comparison of MTF of 5D, D700 and V550 in LP/PH.

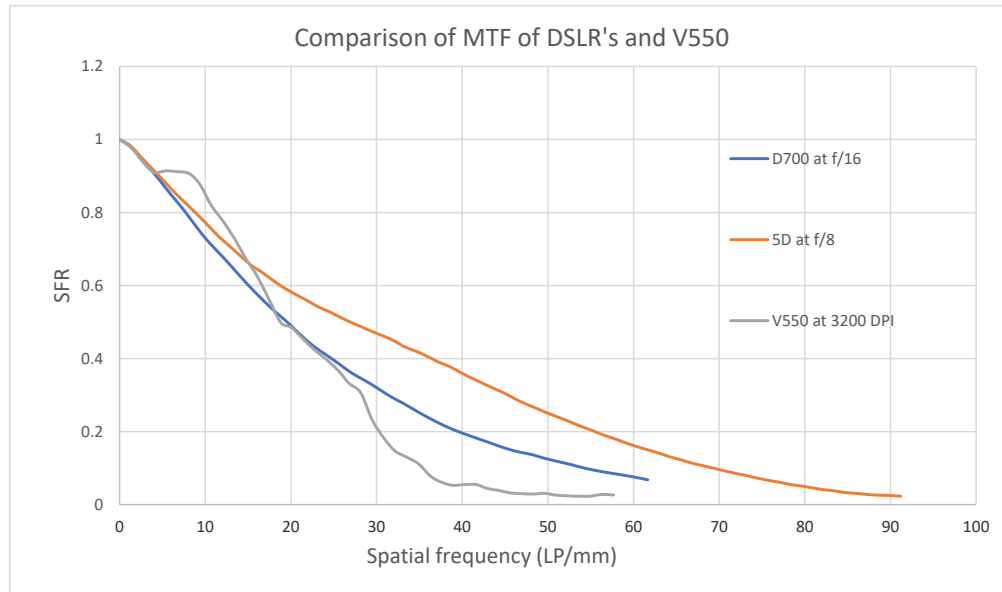


Figure 6.5.6: Comparison of MTF of 5D, D700 and V550 in LP/mm.

Both DSLRs outperformed V550 in terms of MTF, especially in high spatial frequencies. 5D is a newer DSLR and was equipped with superior optics designed for macro photography, thus having the best SFR of all above devices.

6.6 System with analog + digital camera

I tested MTF and OECF of a system that first used an analog camera (Canon AE-1 Program), and then digitized film from that camera using a digital camera (Canon EOS 5D Mark IV), to see how it would perform as a whole. However, I was then offered to include a dedicated film scanner, *Nikon Coolscan IV*³⁹, in my work. Evaluating MTF of that device with FSR2 from Danes Picta would prove impossible, as it is in the same casing as the TSD28 in figure 6.4.1, but Coolscan IV only accepts bare film. Furthermore, the film strip needs to contain 2 to 6 images, however FSR2 is a single image. In this situation, I used a developed Fomapan 100 film strip that contained a photograph of transparent glass chart from Danes Picta based on ISO 12233 norm⁴⁰ (scan from

³⁹<https://imaging.nikon.com/lineup/scanner/coolscan-4/>

⁴⁰<https://www.iso.org/standard/71696.html>

V550 shown below on figure 6.6.1). This chart allowed me to compare Coolscan IV to 5D and V550 in terms of MTF.

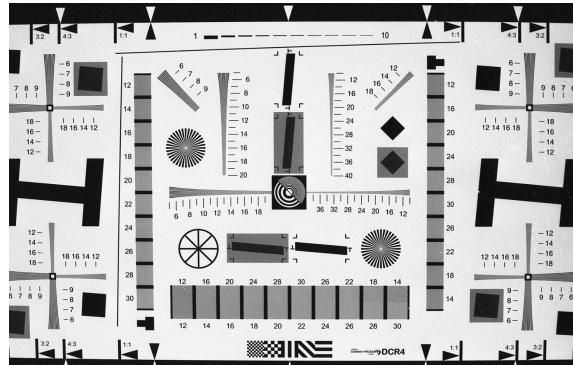


Figure 6.6.1: Figure of transparent glass chart from Danes Picta, adhering to ISO 12233 norm. Scanned by Epson V550.

Coolscan IV is a device from 2006, and the only way I was able to operate it was through installing *Nikon Scan 4* software + drivers for Windows Vista from their website⁴¹, although it stopped responding frequently. The test chart was taken on negative film and then developed, so it contained grain and the results were further affected by the AE-1's own MTF. Comparison is shown in figure 6.6.2 in LP/PH and 6.6.3.

⁴¹https://www.nikoningsupport.com/eu/BV_article?articleNo=000043174&configured=1&lang=en_GB

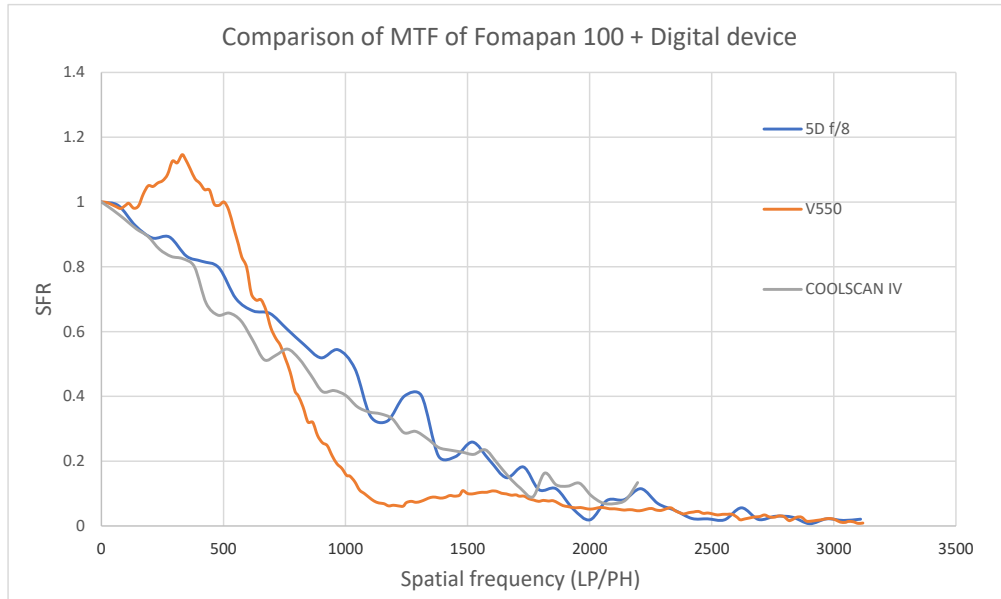


Figure 6.6.2: Comparison of MTF of 5D, V550 (4800 DPI) and Coolscan IV (2900 DPI) scanning Fomapan 100 in LP/PH.

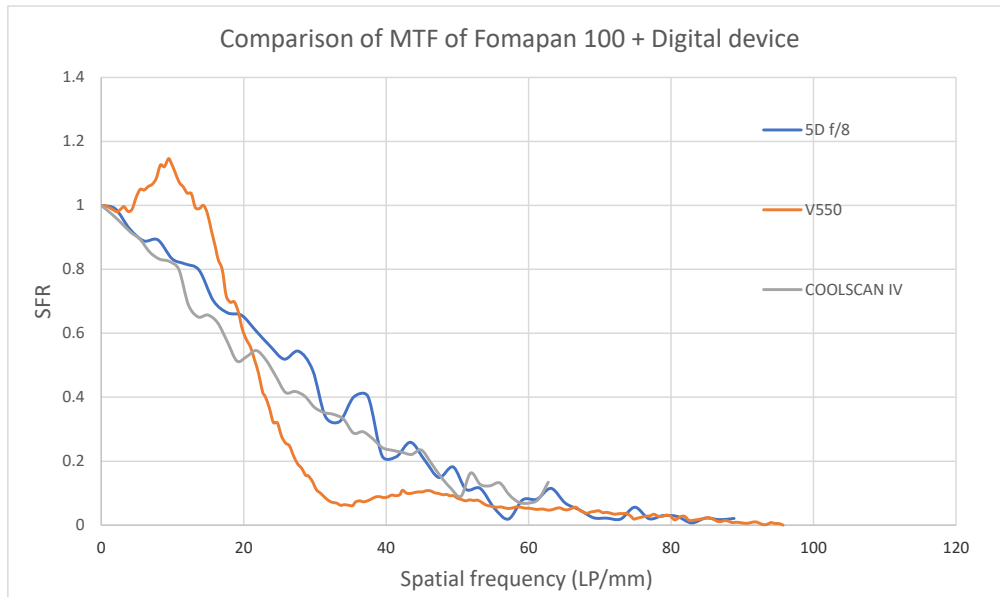


Figure 6.6.3: Comparison of MTF of 5D, V550 (4800 DPI) and Coolscan IV (2900 DPI) scanning Fomapan 100 in LP/mm.

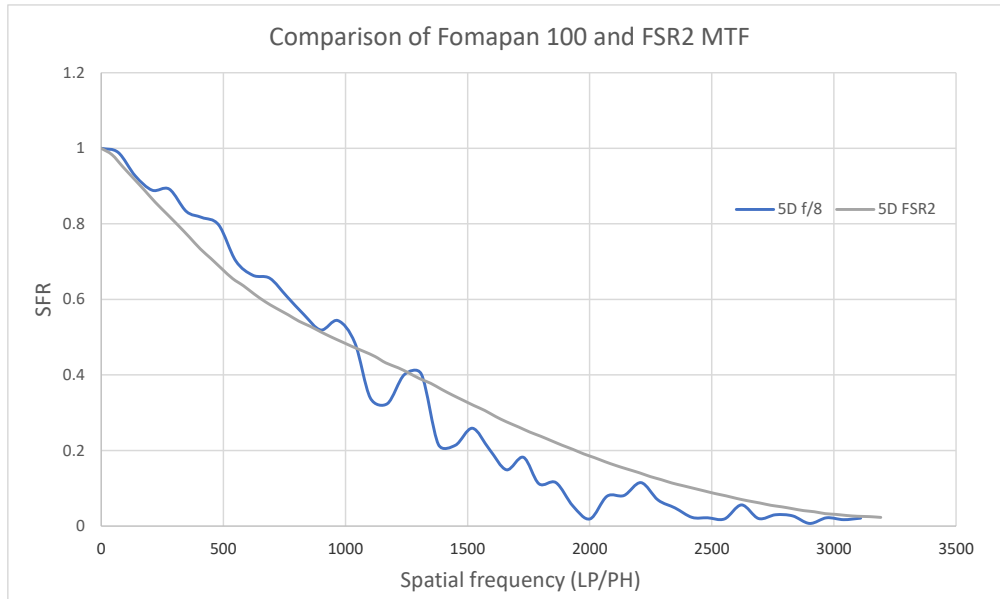
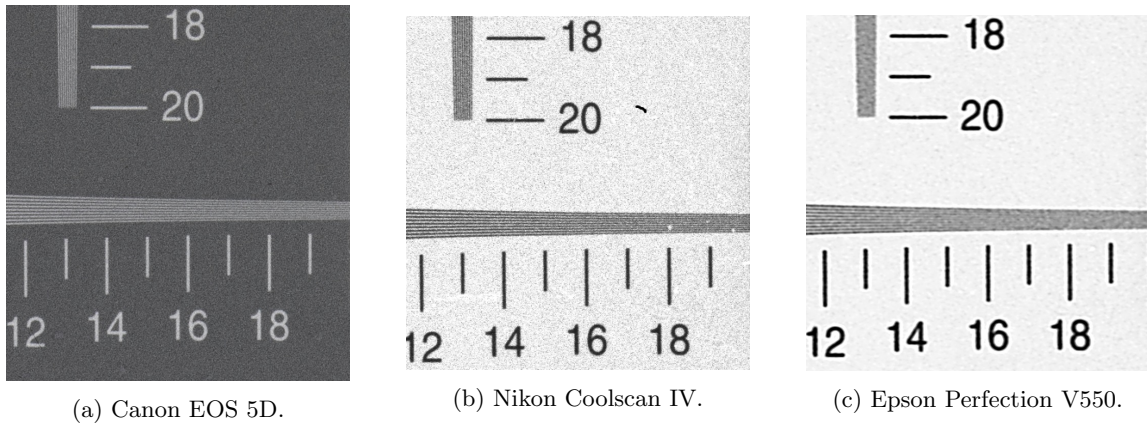


Figure 6.6.4: Comparison of MTF of 5D using FSR2 chart and ISO 12233 chart on Fomapan 100.

MTF chart shows that V550 underperforms in higher frequencies, while Coolscan IV and 5D are tied in that regard. For illustration/subjective evaluation, see figure 6.6.5, where I compare 5D, V550 and Coolscan IV. With a glance, it's perceptible that V550 can not capture high spatial frequencies as well as Coolscan IV or 5D. An important question is whether that is caused by the similar capabilities digital devices, or limitations of the analog camera. To try and answer that, I compared both data sets for 5D, as shown in figure 6.6.4, and it seems that FSR2 scan is better in mid-high frequencies. Coolscan IV has an additional option in post-processing to use Digital ICE, removing scratches and dust, however, it did not work in my case. The darker regions became completely black and the dust and scratches were still apparent.



(a) Canon EOS 5D.

(b) Nikon Coolscan IV.

(c) Epson Perfection V550.

Figure 6.6.5: Visual comparison of 5D, V550 (4800 DPI) and Coolscan IV (2900 DPI).

For OECF (script *OECF2.m*), I used the ISO 14524⁴² OECF test chart with a luminance ratio of 1000:1, which was as well manufactured by Danes Picta (shown in figure 6.6.6). Per the standard, densities for luminance ratio of 1000:1 are defined in a manner which is in the following table (6.4). It also contains measured luminance in $\frac{\text{cd}}{\text{m}^2}$, which should correlate with transmittance. This data was acquired by means of a spectroradiometer *Konica Minolta CS-2000*⁴³. It operated from a distance of approximately 0.63 m (same distance from which AE-1 took the photograph in the first place), observing an angle of 1° .

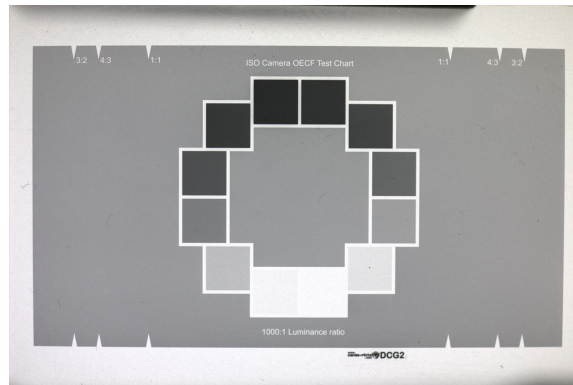


Figure 6.6.6: ISO 14524 test chart, photographed on Fomapan 100 by Canon AE-1 Program, and digitized with Canon EOS 5D Mark IV. It was linearly inverted in MATLAB, then OECF was measured.

⁴²<https://www.iso.org/standard/43527.html>

⁴³<https://www.pro-lite.co.uk/File/CS-2000.php>

Patch	Density	Luminance ($\frac{\text{cd}}{\text{m}^2}$)
1	0.10	1604
2	0.21	1197
3	0.33	924
4	0.47	652
5	0.62	479
6	0.79	314
7	0.98	205
8	1.21	122
9	1.48	68
10	1.84	25.6
11	2.32	10.1
12	3.1	2.2

Table 6.4: Table containing densities and measured luminances of ISO 14524 1000:1 test chart.

Figure 6.6.7 below shows the OECF of gamma-corrected and inverted digital scan from 5D, including noise characteristics of this system. The AE-1 Program along with 5D have encompassed a density range of **2.31 D** per definition of OECF, it does not clip in the highlights, and S/N falls below 1 at $D = 3.1$.

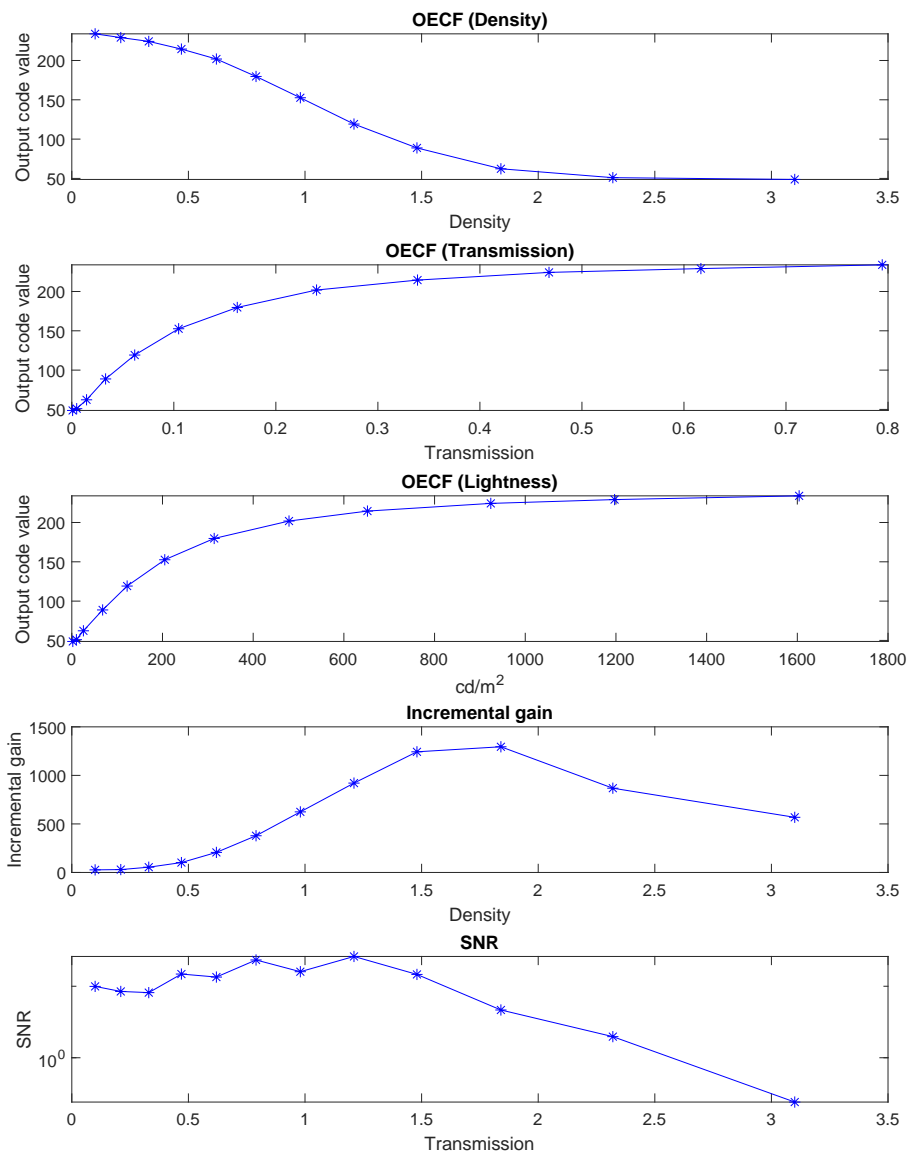


Figure 6.6.7: OECF measurement of system compiled of AE-1 Program and 5D, including noise characteristics.

7 Linear density encoding and digital printing

This section first demonstrates my proposed process of linear density encoding and its implementation, and then demonstrates how that encoding can be used to emulate a printing process digitally, if provided with information about photographic paper.

7.1 Transfer function for linear density encoding

Let's call CV_{in} the input CV of the log transformation, CV_{out} the output CV of the log transformation. $k_{1,2}$ are constants. The transformation will then have the following form

$$CV_{out} = k_1 \cdot \log_{k_2} (CV_{in} + 1). \quad (7.1.1)$$

The $+1$ in the equation above ensures that 0 gets mapped to 0. As is apparent from the log identity $\log_a b = \frac{\log_c b}{\log_c a}$, the linearity of density won't be affected by base of the logarithmic transfer function, nor by any constants in it before it. Base k_2 can be included in coefficient k_1 due to the identity. Those constants will however have an effect on the slope of the density to CV relationship, or $S = \frac{\Delta D}{\Delta CV}$. Obviously, we want a small enough S so that the increments in density are not perceptible (something that is unlikely to happen anyway, because of the high amount of quantization steps in 16 bits). To achieve a small S , we need to ensure that the output CVs (CV_{out}) of the transformation occupy enough of the 16-bit space. Therefore, the choice of base/coefficients of the log transform need to ensure 2 things: that no possible potential densities are clipped, and that the quantization step of densities S is small enough. Ideally, we'd use all of the available space in 16 bits and the situation would be $CV_{in}(0) = CV_{out}(0) = 0$ and $CV_{in}(2^{16} - 1) = CV_{out}(2^{16} - 1) = 2^{16} - 1$. For example a transfer characteristic that would closely approximate this is

$$CV_{out} = 13600 \cdot \log_{10} (CV_{in} + 1). \quad (7.1.2)$$

I came to those coefficients by setting k_2 to 10 and gradually adjusting k_1 . This transfer characteristic uses virtually all of the 16-bit space, as $2^{16} - 1 = 65,535$ is mapped to 65,504. But we must keep in mind, we may need to stretch those values later when converting from log. exposure to densities of photographic paper (described in detail in section 7.3), so to avoid clipping during that phase, we must choose a slightly lower value, or work in a higher bit-depth (floating point).

Once the transformation is done, we need a way to determine the used density range and a way to read densities from CV_{outs} . To do that, we need to keep track of where the CVs of D_{max} and D_{min} are mapped. I will do that by transforming the data obtained from the OECF calibration chart, we will know D_{max} and D_{min} as well as $CV_{out}(D_{max})$ and $CV_{out}(D_{min})$. Assuming that the relationship between CV_{out} and densities is linear, everything between D_{max} and D_{min} is also linear and we can therefore calculate any other point positioned between them. I will use the slope S to do following

$$S = \frac{D_{max} - D_{min}}{CV_{out}(D_{max}) - CV_{out}(D_{min})}. \quad (7.1.3)$$

To then obtain the density value of any particular output CV, let's say $CV_{out}(x)$, this is done

$$D(CV_{out}(x)) = D_{min} + S \cdot [CV_{out}(x) - CV_{out}(D_{min})]. \quad (7.1.4)$$

I took the step S , multiplied it by the amount of CVs between $CV_{out}(D_{min})$ and $CV_{out}(x)$, and added it to D_{min} . We also might need to orient ourselves in the opposite direction, find a corresponding CV of a density value ($D(x)$)

$$CV(D(x)) = D_{min} + \frac{1}{S} \cdot [D(x) - D_{min}]. \quad (7.1.5)$$

Finally, when it is needed, inverse transformation is calculated in the following fashion

$$CV_{in} = k_2 \frac{CV_{out}}{k_1} - 1. \quad (7.1.6)$$

7.2 Process of linear density encoding

I made a flowchart on which I based a MATLAB script, shown on figure 7.2.1. First, all necessary **RAW images** are taken with a camera and transformed into a **16-bit TIFF with baked in white balance**. Those images contain the scanned film itself, a calibration chart for OECF and a flat-field photograph. To counter uneven illumination and vignetting, **flat-field correction** (section 6.3) is performed on scanned film and calibration chart files. If the calibration chart was taken with different camera settings than the scanned film, it can be **exposure compensated**, i.e., if the chart image used 1 s exposure time, the film used 0.5 s, and the ISO + f-number were same, then the linear data in the film image must be multiplied by 2. It's reasonable to assume, however, that precautions will be taken to ensure these photos are taken with the exact same camera settings. Data from the calibration chart image is used to measure **OECF** and thus D_{max} and D_{min} , those are used to establish **transfer function coefficients**, making sure that no necessary values are clipping. Data from the scanned film image is then logarithmically encoded to contain **linear density representation**. Below are figures containing the samples and their logarithmically encoded versions, with histograms.

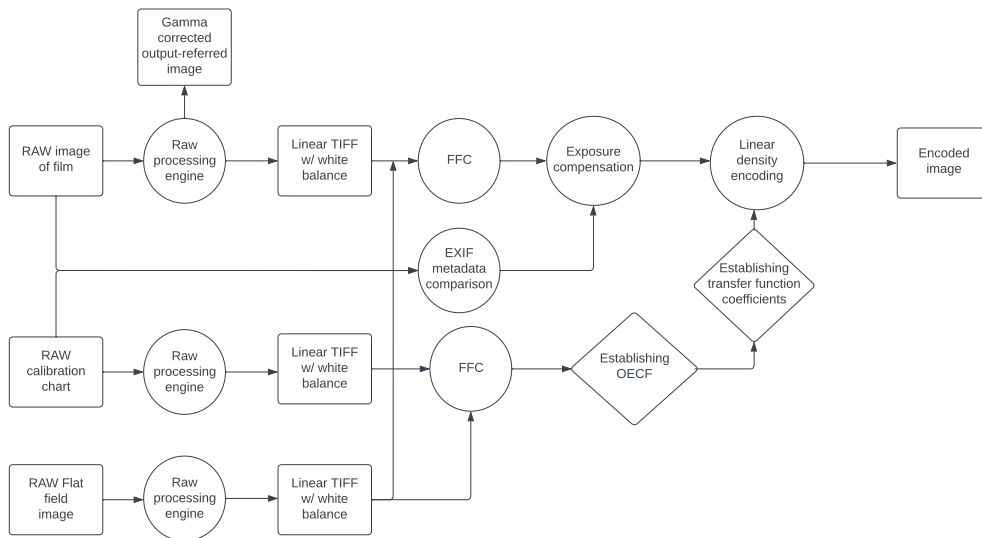


Figure 7.2.1: Proposed process for linear density encoding

7.3 Proposed digital printing process

In section 2.7.3, I proposed a digital printing process, where a film is digitized and then a printing process is simulated digitally, using data about a real photographic paper.

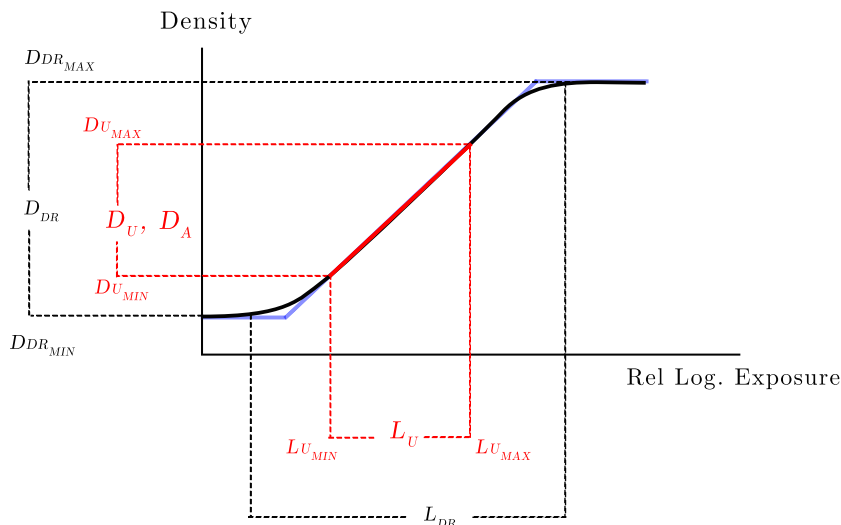


Figure 7.3.1: Illustration of typical print/photographic paper characteristic curve and variable names I will use in this section. Black line is the characteristic curve, red line represents values that hold visual information (which in this case is not clipping), and blue line would potentially clip values based on D_{DR} and γ_{film} of the photographic paper. Inspired by the negative Fomaspeed paper mentioned in the footnote.

An example of a photographic paper is the Fomaspeed, with its datasheet in the footnote⁴⁴. The characteristic curves of print paper (film in general) are log-log, they have 2 logarithmic axes, and a substantial portion of the curve is often linear. The horizontal axis is either in a decadic (logarithmic exposure) or a binary (stops) logarithm. For convenience, I find it practical to convert everything into a decadic logarithm (because density is a decadic logarithm), so we will need to use a log identity to convert from stops: $\log_{10} x = \frac{\log_2 x}{\log_2 10}$. Change of logarithm base is multiplying by a constant, so it essentially changes the slope of the linear portion and very little else. This identity also points out that the base of the logarithm or a multiplicative coefficient before the logarithm do not affect the linearity of density - if linear transmission data is somehow logarithmically encoded, the result will be linearly encoded density.

Transmittance and density only by themselves amount to nothing unless there is a light source present in our case. To establish a relationship for finding log exposure from density, let's assume a light source with intensity I , a medium with transmittance T (density D) and some coefficient C , which alters the exposure time. The amount of light passing through this medium is then

⁴⁴<https://www.foma.cz/cs/fomaspeed>

$C \cdot I \cdot T = C \cdot I \cdot 10^{-D}$. In logarithmic scale, that will be $\log_{10}(10^{-D} \cdot C \cdot I) = -D + \log_{10} C + \log_{10} I$, so it is inverse density plus some added constants. Since we need *relative* log. exposure, the numerical values of these constants are irrelevant. In this work, I will map density onto logarithmic exposure based on the optimal positioning on the characteristic curve, one where no/minimal values would clip. On figure 7.3.1, the red color represents areas with visual information and the figure itself depicts a situation where we don't have to clip it. However, the density range of the printing paper may be less than necessary to store all visual information, and if we desire to estimate the look of the photographic paper, we must clip the values not in the dynamic range of the paper (D_{DR}).

I would like to clarify the terms I will use further - dynamic range (subscript DR) means the entire available range that can be used to store visual information, while used range (subscript U) is the range that actually contains visual information and includes that information in the variable. I will write the max and min values with suffixes as well (e.g., $D_{DR_{max}}$, $D_{U_{max}}$). They are illustrated on 7.3.1. The image shows non-linear portions of the graph as well, but those will be hard to estimate given only a characteristic curve, so I will extend the linear portion until the values clip (blue curve).

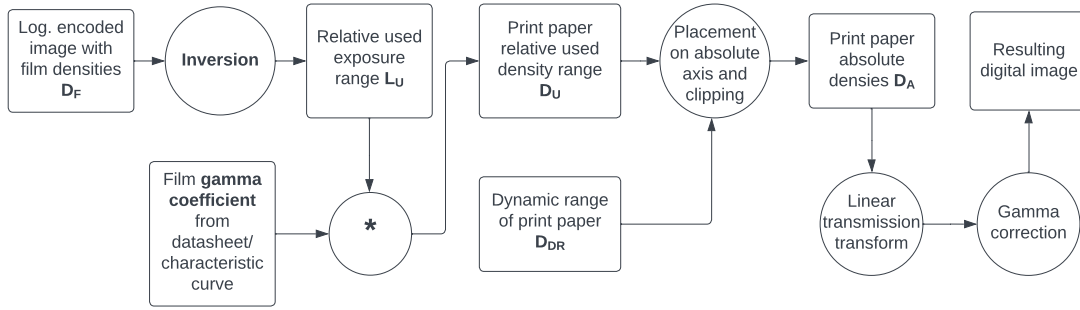


Figure 7.3.2: Proposed digital printing process.

The digital printing process I propose requires establishing the relative D_U , selecting a position on the characteristic curve to place it on, and clipping values outside D_{DR} , (density range of the printing paper is limited, that must be respected). The block diagram 7.3.2 shows the whole process. At first, I will use the **logarithmically encoded film density** D_F and use it to find the used **relative log. exposure range**, ($L_U = L_{U_{max}} - L_{U_{min}}$) using **inversion** (perhaps Max. possible $CV - D_F$). To determine the **relative used density range of the printing paper**, we will need the gamma coefficient, $D_U = \gamma_{film} \cdot L_U$, this operation stretches/compresses the used range. Once we do that, we must place this relative D_U somewhere on the absolute density axis of the print paper, preferably so that no/minimal values are clipping. At this point, having projected the log. exposure onto density using the characteristic curve, we should have a positive log. encoded image which represents the **absolute densities on the printing paper**, D_A . If we wish to view the result on a digital monitor, then the last step would be **inverse logarithmic transformation**, from linear density representation to linear transmission/opacity representation, **and gamma correction**, since the original data from which D_F is obtained is linear.

The above process applies to B&W film. For color film, it would be similar, although more complicated due to 3 color components instead of 1. First, after the linear images are acquired with spectral conditions specified in ISO Status M/A, each color component is log. transformed separately, transformed into log. exposure separately and mapped onto printing paper densities separately. Each color-forming dye of the a photosensitive material has a slightly different characteristic curve, the film gamma γ_{film} visually tends to be the same [21], [22], but the densities created by exposing those layers to the same light intensity and exposure time are different, and those relative ratios must be respected. The optimal spectral composition of the illuminating light source is often specified in the datasheet of the printing paper.

7.4 Encoding and printing process

Following was done using the *transforms.m* MATLAB script. I first entered parameters of the photographic paper, Fomaspeed 100⁴⁵ and chose a log. exposure range of ISO R 120 ($D = 1.2$). I then loaded an OECF image taken with 5D, at **1/8 s** and **f/5.6** and selected 28 patches to establish the D_{min} and D_{max} can handle, and calculated then slope S to reach any density needed from those extremes (for example D_{min} and D_{max} of the paper). After that, the script loads the two linear images to be encoded (taken with the exact same camera settings), transforms them into grayscale and then into double-precision floating point to avoid rounding errors during transformations. To display any intermediate and final images, I used the *uint16* function to convert them back into 16-bit unsigned integer (space of 16-bit TIFF). The process used following transformation

$$CV_{out} = 6800 \cdot \log_{10}(CV_{in} + 1). \quad (7.4.1)$$

The coefficient k_1 was chosen as 6800 to avoid unnecessary clipping during later stages of this script. Original linear images of guitars and castle, along with their manually edited and log. encoded variants can be seen in figures 7.4.1 and 7.4.2 below. The encoded image is D_F .

⁴⁵<https://www.foma.cz/cs/fomaspeed>

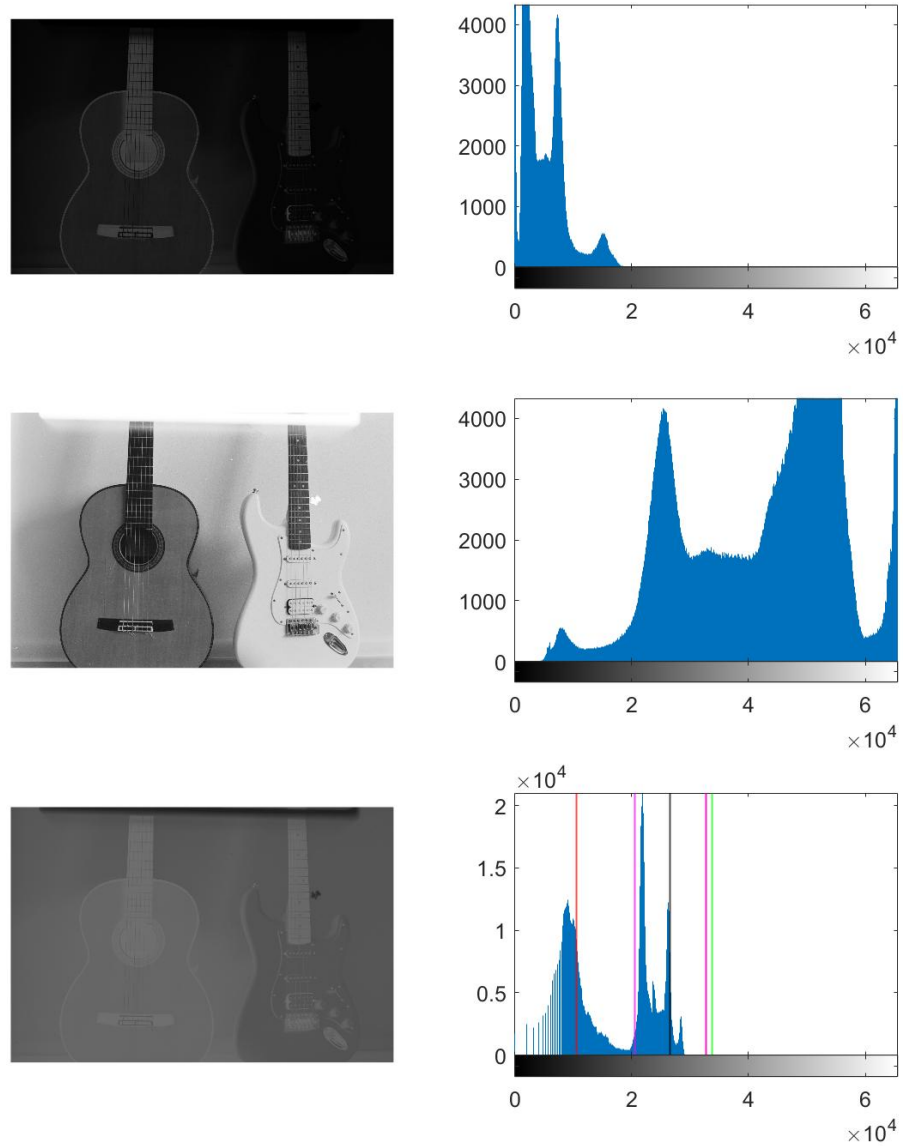


Figure 7.4.1: Linear, manually edited and log. transformed images of guitars with histograms. Red lines show density extremes of the system (0.15 - 0.68), purple lines show density extremes of the photographic paper (0.15 - 2.1) and black line shows mean density of the paper. The green line is a density of 0 - no values were scanned above that.

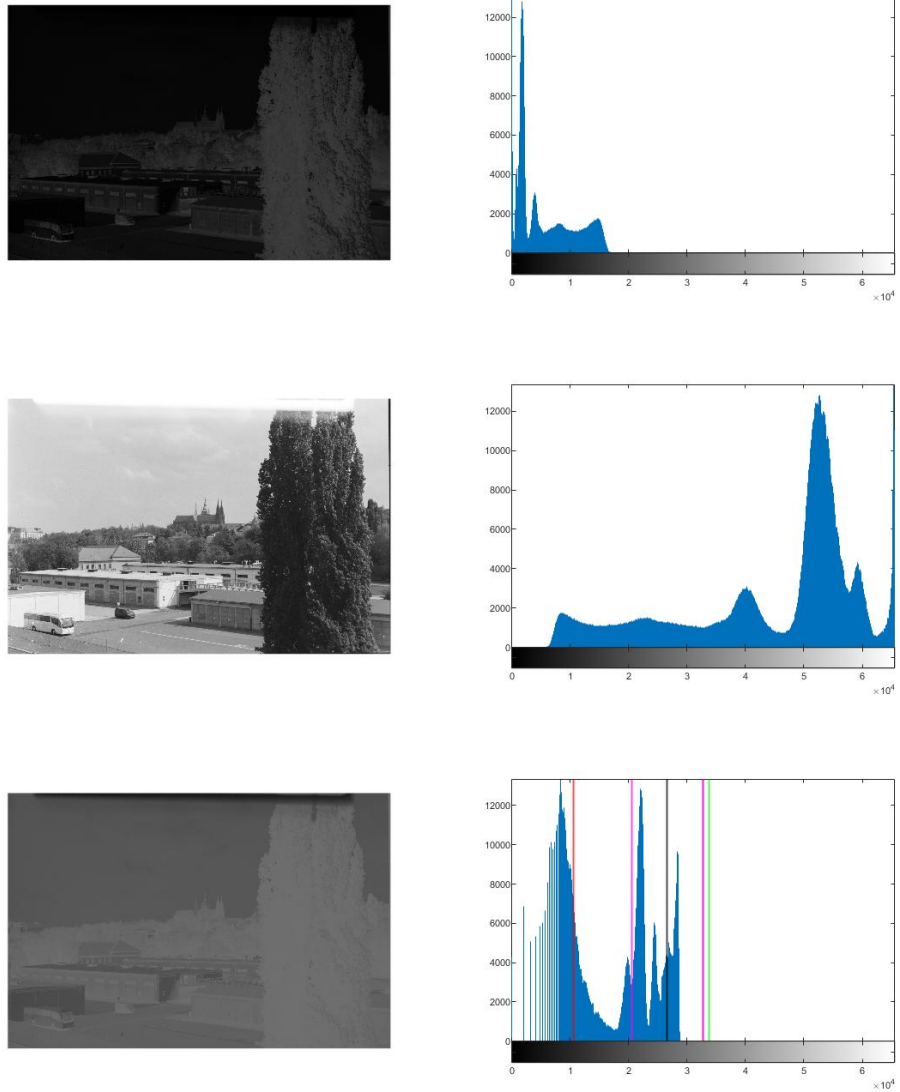


Figure 7.4.2: Linear, manually edited and log. transformed images of castle with histograms. Red lines show density extremes of the system (0.15 - 0.68), purple lines show density extremes of the photographic paper (0.15 - 2.1) and black line shows mean density of the paper. The green line is a density of 0 - no values were scanned above that.

Looking at the bottom histograms, we are already beginning to see a potential hazard to log. encoding - perceptible banding in dark areas. The next step is to invert the images, I did this by subtracting the image matrices from maximum uint16 value, or $2^{16} - 1$, and subtracting further to shift the histogram fully to the left (without clipping). Inverted images as well as histogram equalized versions of them (for illustration) are in figure [7.4.3](#), and those inverted images as this stage are L_U .

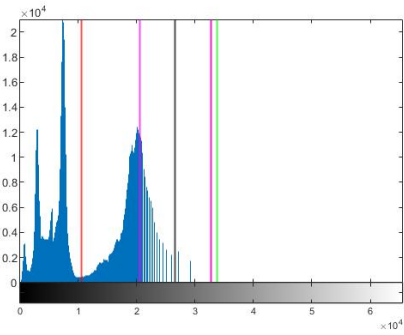
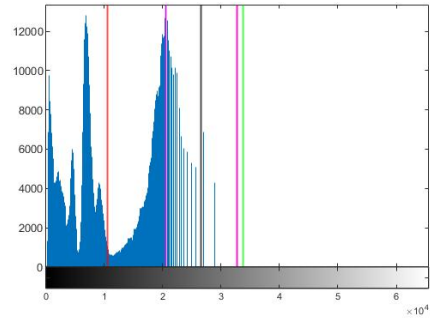


Figure 7.4.3: Inverted and histogram equalized images of guitars and castle. Red lines show density extremes of the system (0.15 - 0.68), purple lines show density extremes of the photographic paper (0.15 - 2.1) and black line shows mean density of the paper. The green line is a density of 0.

The image is inverted and the banding has now been moved to the right side of the histogram, into the highlights. The rest is unchanged. Histogram equalized images show that the data is still usable. The next step in the process is multiplying the image by gamma. I first added 1 to the matrix, so that values of 0 do not stay unchanged. I subtracted it after. At this scale, this step is not necessary, but it is correct. I calculated the print paper's gamma as the density range of the paper divided by log. exposure range: $\gamma = \frac{2.1-0.15}{1.2}$, and subsequently multiplied the image matrix by that value, stretching it (this is why we can not initially use the full range of 16-bit space, the image could get clipped). Now we have reached D_U and the absolute densities do not yet matter, because we are dealing with *relative* logarithmic exposure converted to densities, shown in figure 7.4.4. All that is left is to do is to place this density information onto the *absolute* density axis, obtain D_A and gamma encode the result ($\gamma = \frac{1}{2.2} \approx 0.45$ so it is displayed correctly. At this point, however, that limitations of this method started to show.

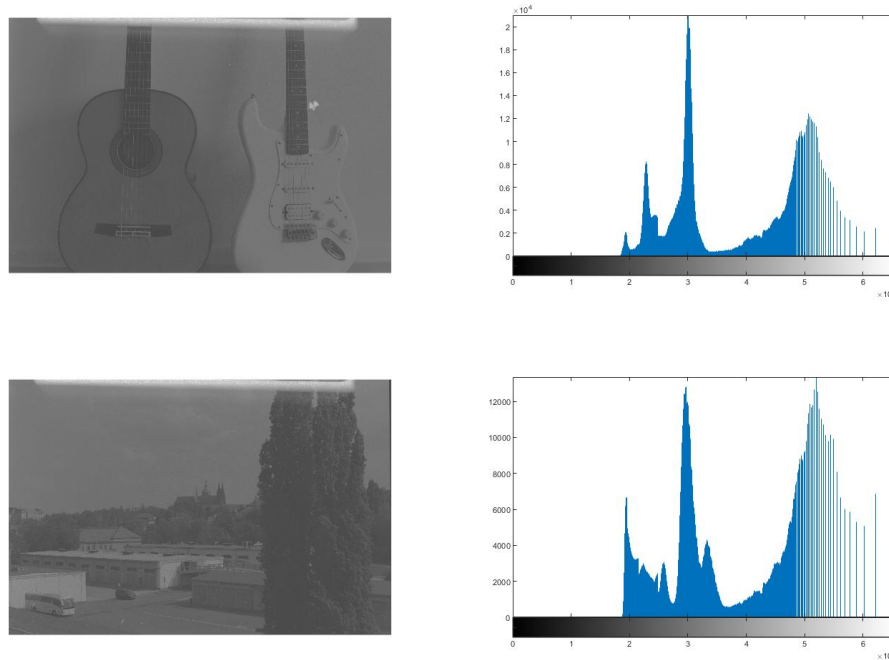


Figure 7.4.4: Images storing the final relative density of the photographic paper.

I did not find a reliable automated method of establishing the right placement of the relative density image onto absolute density axis. I tried finding a mean of D_U relative density images, and aligning it with the mean of the photographic paper density, then I tried the same with medians, however the final image was unacceptable - it was clipping, with almost all values near the extreme edge of the histogram (either almost black or white), because the log and power-law transformations are extreme and the placement in the histogram has to be precise. If the photograph contains an

object that is not related to film, e.g. dirt or a piece of equipment, it may be registered as a density value that can't be even reproduced by the film, and when inverted, will offset the true min. density (max. CV) in the image. The only remotely acceptable result was when I prevented highlights from clipping - I shifted the image histograms fully to the right, as is seen in figure 7.4.5.

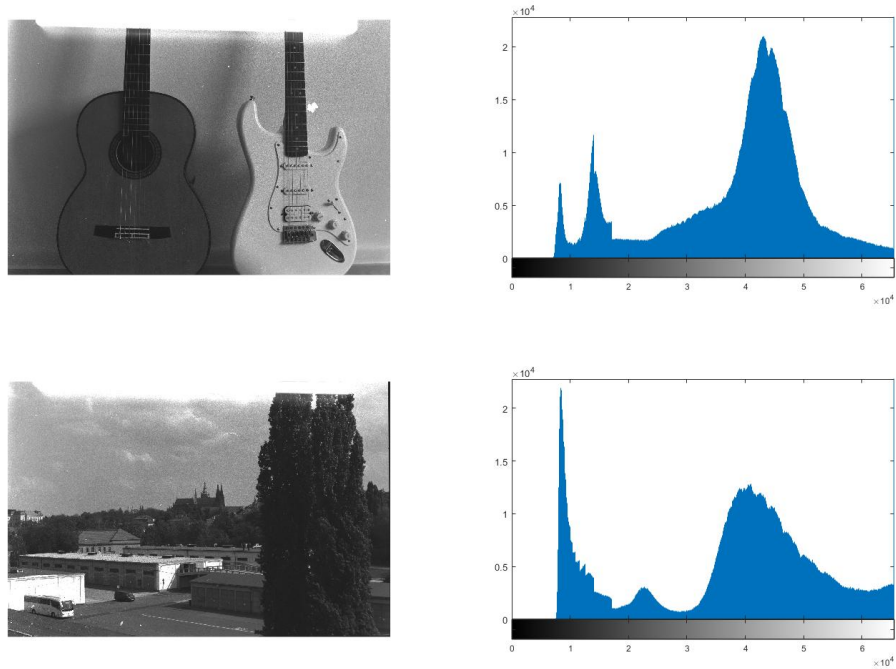


Figure 7.4.5: Inverse transformed and gamma encoded images of guitars and castle.

It is evident, however, that a lot of pixels are still clipping, and this method of also placement fully depends on the k_1 coefficient, as that coefficient has a direct impact on the width of the images in the histogram, e.g., if the image is too narrow, it will not have any dark tones. Changing the coefficient to lower or higher values rendered the final image unusable. The only workaround is to adjust the 'illumination intensity' manually, which is manifested as *exposure* variable in the beginning of the script. It directly adds CVs to the inverted log. encoded image containing D_U , just like adjusting exposure time in real life (in the logarithmic domain, multiplication becomes addition). My proposed method and its implementation successfully allowed for accurately linearly encoding densities and storing them in an image, but did not give fully positive results when trying automate digitally printing the scanned material onto a photographic paper.

8 Conclusions

The assignment was to provide overview about possible methods of digitization of film, mainly those using a digital camera. Using the information about those methods, it was necessary to implement tools for evaluation of performance of said methods, and to implement tools for post-processing of scanned samples using those methods.

In the work, I summed knowledge about digital imaging required to digitize film, and described existing methods of digitizing film using a DSLR, as well as tools, parameters and standards used to digitize motion picture film with dedicated film scanners. Based on the Cineon process, which emulates how a print stock would see film, I proposed encoding RAW files logarithmically, so they contain linear data about density. Using encoded images, I then came up with digital printing. Assuming that a digital camera will not capture the dynamic range of positive film in its entirety, I summed up a comparison of HDR storage methods, where Radiance XYZE and OpenEXR formats seem like optimal solutions for storing HDR images of digitized film. A brief discussion about optical aberrations and their possible corrections followed.

For measurements and demonstrations, I used a full-frame *Nikon D700* camera with zoom lens and extension rings, and a full-frame *Canon EOS 5D Mark IV* with macro lens. First setup involved the D700 on a tripod and a large slanted illumination stand. This setup allowed for good dynamic range, but poor focus. On the contrast, second setup with D700 on a rail system allowed for better alignment of sensor and film, but did suffer from light spill. Third setup used 5D and rail system, it had both good focus and dynamic range, but light spill still affected the results. To compare the performance of DSLR to a typical flatbed scanner, I also used an Epson Perfection V550 to scan a density calibration sheet and MTF measuring sheet. For comparison to a typical dedicated film scanner, I used Nikon Coolscan IV, and compared it to 5D and V550.

Based on the data from three measurements, I established the OECF and MTF of the scanning setups using DSLR. Data about OECF shows that the dynamic range of SDR DSLR scanning is larger than that of the flatbed scanner, and there was no advantage in using HDR merging to increase the dynamic range throughout this work - in one case of HDR, the dynamic range was identical to SDR (3.53), and in the other, it was worse, same as the scanners (3.41).

In MTF measurements, both cameras placed above the Epson V550 as well. I measured the effect of f-number on the MTF for 5D, from $f/4$ to $f/16$, and best results in high spatial frequencies were obtained using $f/8$ and $f/11$ apertures. While comparing the 5D to Coolscan IV and V550 using a digitized film image of ISO 12233 taken with *Canon AE-1 Program*, V550 was not able to capture high frequencies as well as 5D or Coolscan IV. The results for the latter two were virtually identical, perhaps suggesting that the visual information in scanned film itself did not contain high enough spatial frequencies.

I further proposed a method of digital printing, where one would log encode a scanned image and further manipulate it to digitally emulate analog printing. It worked, up to a point where inverse transformation had to be applied - the final results were not acceptable. Using two samples and the OECF of a SDR DSLR image, I was able successfully to implement a logarithmic intensity transformation for linear encoding of densities. It proved difficult to find a reliable and consistent

automated method of inverse transforming the log. encoded and manipulated images, I had to manually adjust exposure to obtain acceptable results.

Attachments

FFC.zip

FFC (Flat-field correction) archive contains an interactive script to perform FFC. Additional files must be downloaded separately. Readme file included.

OECECF.zip

OECECF (Opto-electronic conversion function) archive contains scripts to perform OECECF and plot it. Additional images must be downloaded separately. Readme file included.

Transform.zip

Transform archive contains MATLAB files to logarithmically encode and digitally print scanned images - a script used to generate images for this work, and an interactive script. Additional images must be downloaded separately. Readme file included.

References

- [1] VES Jeffrey A. Okun and VES Susan Zwerman. *The VES Handbook of Visual Effects: Industry Standard VFX Practices and Procedures*. Taylor & Francis, 2020. ISBN: 9781351009393. URL: <https://books.google.cz/books?id=VsXrDwAAQBAJ>.
- [2] M. Rabiger and M. Hurbis-Cherrier. *Directing: Film Techniques and Aesthetics*. Taylor & Francis, 2020. ISBN: 9781351186377. URL: <https://books.google.cz/books?id=se7QDwAAQBAJ>.
- [3] Marek Jícha et al. *Živý film: Digitalizace Filmu Metodou Dra*. Lepton studio, 2016.
- [4] R. Sheppard. *Adobe Camera Raw for Digital Photographers Only*. For Only. John Wiley & Sons, 2008. ISBN: 9780470224571. URL: <https://books.google.cz/books?id=Wp1DMbJadioC>.
- [5] *How Scanners Work*. URL: <http://preservationtutorial.library.cornell.edu/tutorial/technical/technicalB-02.html> (visited on 05/17/2022).
- [6] Phase One. *Cultural Heritage: Solution guide*. 2020. URL: https://digitization.phaseone.com/wp-content/uploads/sites/4/2020/12/Solution_Guide_2020_July.pdf (visited on 05/17/2022).
- [7] MATLAB. *Enhance contrast using histogram equalization*. 2022. URL: <https://www.mathworks.com/help/images/ref/histeq.html> (visited on 05/17/2022).
- [8] Harald Brendel. *The ARRI Companion to Digital Intermediate*. 2005. URL: http://dicomp.arri.de/digital/digital_systems/DIcompanion/index.html (visited on 03/27/2022).
- [9] Cambridge in colour. *Understanding gamma correction*. 2020. URL: <https://www.cambridgeincolour.com/tutorials/gamma-correction.htm> (visited on 05/17/2022).
- [10] ARRI. *Log C*. URL: <https://www.arri.com/en/learn-help/learn-help-camera-system/camera-workflow/image-science/log-c> (visited on 05/17/2022).
- [11] Nick Carver. *Comparing Film Scans: Drum vs Flatbed vs DSLR*. 2020. URL: <https://www.youtube.com/watch?v=Q9d8BukUgzI&t=1485s> (visited on 05/17/2022).
- [12] Kyle McDougall. *Film Scanning with a Digital Camera — How good is it?* 2022. URL: <https://www.youtube.com/watch?v=00XNCJqJFrc&t=114s> (visited on 05/17/2022).
- [13] KAMERA STORE. *Complete Scanning Kit*. URL: <https://kamerastore.com/products/complete-kit> (visited on 05/17/2022).
- [14] *Negative Lab Pro*. URL: <https://www.negativelabpro.com/> (visited on 05/17/2022).
- [15] DT. *Phase One IQ4 150MP Camera System*. URL: <https://www.digitaltransitions.com/product/phase-one-iq4-150mp-system/> (visited on 05/17/2022).
- [16] DT. *45mm LS f/3.5 Blue Ring*. URL: <https://dtcommercialphoto.com/product/45mm-ls-f3-5-blue-ring/> (visited on 05/17/2022).
- [17] KAISER. *Kaiser Copylizer*. URL: https://www.bhphotovideo.com/c/product/1480006-REG/kaiser_205215_copylizer_executive_hf_led.html (visited on 05/17/2022).
- [18] PhotographyMad. *Macro Lenses*. URL: <https://www.photographymad.com/pages/view/macro-lenses> (visited on 05/17/2022).

- [19] Masterclass. *Complete macro photography guide for beginners*. 2020. URL: <https://www.masterclass.com/articles/complete-macro-photography-guide-for-beginners#what-is-the-best-camera-for-macro-photography> (visited on 05/17/2022).
- [20] Richard Patterson. “For Scanning Negative”. In: (2007).
- [21] Kodak. *KODAK PROFESSIONAL EKTAR 100 Film*. 2016. URL: https://imaging.kodakalaris.com/sites/default/files/files/products/e4046_ektar_100.pdf (visited on 03/27/2022).
- [22] Kodak. *KODAK EKTACHROME 100D*. 2022. URL: <https://www.kodak.com/content/products-brochures/Film/KODAK-EKTACHROME-100D-COLOR-REVERSAL-FILM-5294-7294-datasheet-EN.pdf> (visited on 03/27/2022).
- [23] Kodak. *KODAK VISION3 500T*. 2022. URL: https://www.kodak.com/content/products-brochures/Film/VISION3_5219_7219_Technical-data.pdf (visited on 03/27/2022).
- [24] E.J. Giorgianni and T.E. Madden. *Digital Color Management: Encoding Solutions*. Biomedical Research Reports. Addison-Wesley, 1998. ISBN: 9780201634266. URL: <https://books.google.cz/books?id=IPZRAAAAMAAJ>.
- [25] Barbara Flueckiger et al. *Investigation of Film Material–Scanner Interaction*. 2018. URL: <http://web.archive.org/web/20080207010024/http://www.808multimedia.com/winnt/kernel.htm> (visited on 03/27/2022).
- [26] Nate Photographic. *Suggested backlight sources for scanning film with DSLR*. 2019. URL: <https://forums.negativelabpro.com/t/suggested-backlight-sources-for-scanning-film-with-dslr/130> (visited on 03/27/2022).
- [27] Harald Brendel. *ARRISCAN color calibration*. 2005. URL: http://dicomp.arri.de/digital/digital_systems/DIcompanion/scannerresponse.html (visited on 03/27/2022).
- [28] ARRI. *ARRI Archive Technologies*. 2013. URL: <https://www.youtube.com/watch?v=GzbTSKLS7-c> (visited on 03/27/2022).
- [29] Richard Patterson. *Understanding Cineon*. 2001. URL: <http://www.digital-intermediate.co.uk/film/pdf/Cineon.pdf> (visited on 03/27/2022).
- [30] Jeremy Selan. *VES: Cinematic color*. 2012. URL: <https://cinematiccolor.org/> (visited on 03/27/2022).
- [31] Hou-Ping Wu et al. “Measurement for opto-electronic conversion functions (OECFs) of digital still-picture camera”. In: *Optoelectronic Imaging and Multimedia Technology*. Ed. by Toru Yoshizawa et al. Vol. 7850. International Society for Optics and Photonics. SPIE, 2010, pp. 272–278. DOI: [10.1117/12.869364](https://doi.org/10.1117/12.869364). URL: <https://doi.org/10.1117/12.869364>.
- [32] Canon. *EOS 5D Mark IV - Canon Log*. 2017. URL: <https://shop.usa.canon.com/estore/marketing/EOS-5D-MARKIV/eos5d-canonlog.html> (visited on 03/27/2022).
- [33] DXOMark. *Canon EOS 5D Mark IV*. 2020. URL: <https://www.dxomark.com/Cameras/Canon/EOS-5D-Mark-IV> (visited on 05/17/2022).
- [34] E. Reinhard et al. *High Dynamic Range Imaging: Acquisition, Display, and Image-Based Lighting*. The Morgan Kaufmann Series in Computer Graphics. Elsevier Science, 2005. ISBN: 9780080478319. URL: <https://books.google.cz/books?id=dH2lRxTg1UsC>.

- [35] D.B. Goldman and Jiun-Hung Chen. “Vignette and exposure calibration and compensation”. In: *Tenth IEEE International Conference on Computer Vision (ICCV’05) Volume 1*. Vol. 1. 2005, 899–906 Vol. 1. DOI: [10.1109/ICCV.2005.249](https://doi.org/10.1109/ICCV.2005.249).
- [36] Euresys. *What is Flat Field Correction?* 2020. URL: https://documentation.euresys.com/Products/Coaxlink/Coaxlink_10_3/Content/03_Using_Coaxlink/functional-guide/flat-field-correction/what-is-ffc.htm (visited on 05/17/2022).
- [37] AZO. *Effect and Implementation of Flat Field Correction of a Spatial Heterodyne Spectrometer*. 2020. URL: <https://www.azom.com/article.aspx?ArticleID=14055> (visited on 05/17/2022).
- [38] Alexander Kokka et al. “Flat-field calibration method for hyperspectral frame cameras”. In: (2019).
- [39] Adobe. *What is Chromatic Aberration?* URL: <https://www.adobe.com/creativecloud/photography/discover/chromatic-aberration.html> (visited on 05/17/2022).
- [40] ISO. *ISO 21550:2004 - Dynamic Range Measurements*. 2020. URL: <https://www.iso.org/standard/35939.html> (visited on 05/17/2022).
- [41] ISO. *ISO 12233:2017 - Resolution and spatial frequency responses*. 2020. URL: <https://www.iso.org/standard/71696.html> (visited on 05/17/2022).
- [42] Peter Burns. *Spatial Frequency Response (SFR): sfrmat*. 2022. URL: <http://burnsdigitalimaging.com/software/sfrmat/> (visited on 05/17/2022).
- [43] *Foto Škoda*. URL: <https://www.fotoskoda.cz/> (visited on 05/17/2022).
- [44] RawTherapee. *Color Management*. 2022. URL: https://rawpedia.rawtherapee.com/Color_Management (visited on 05/17/2022).
- [45] FADGI. *Technical Guidelines for Digitizing Cultural Heritage Materials*. 2016. URL: http://www.digitizationguidelines.gov/guidelines/FADGI_Still_Image_Tech_Guidelines_2016.pdf (visited on 05/17/2022).
- [46] Canon. *Make the Transition to Black and White Digital Photography*. 2017. URL: <https://www.usa.canon.com/internet/portal/us/home/learn/education/topics/article/2018/June/Make-the-Transition-to-Black-and-White-Digital-Photography/Make-the-Transition-to-Black-and-White-Digital-Photography> (visited on 03/27/2022).